LA-4057-MS

LOS ALAMOS SCIENTIFIC LABORATORY
of the
University of California
LOS ALAMOS • NEW MEXICO

CMF-13 Research on Carbon and Graphite

Report No. 7

Summary of Progress from
August 1 to October 31, 1968

UNITED STATES
ATOMIC ENERGY COMMISSION
CONTRACT W-7405-ENG. 36

Distributed December 31, 1968

LA-4057-MS
SPECIAL DISTRIBUTION

LOS ALAMOS SCIENTIFIC LABORATORY
of the
University of California
LOS ALAMOS • NEW MEXICO

CMF-13 Research on Carbon and Graphite

Report No. 7

Summary of Progress from August 1 to October 31, 1968*

by

Morton G. Smith

*Supported in part by funds transferred by NASA through the joint AEC-NASA Space Nuclear Propulsion Office, and directly from the NASA Office of Advanced Research and Technology.

CMF-13 RESEARCH ON CARBON AND GRAPHITE
REPORT NO. 7: SUMMARY OF PROGRESS FROM AUGUST 1 TO OCTOBER 31, 1968

I. INTRODUCTION

This is the seventh in a series of progress reports devoted to carbon and graphite research and development in LASL Group CMF-13, and summarizes work done during the months of August, September and October, 1968. It should be understood that in such a report many of the data given are preliminary, incomplete, and subject to correction, and that many of the opinions and conclusions stated are tentative and subject to change. This report is intended only to provide up-to-date background information to those who share the interests of the programs described in it, and should not be quoted or used as a reference publicly or in print.

Research and development on carbon and graphite were undertaken by CMF-13 primarily to increase understanding of their properties and behavior as engineering materials, to improve the raw materials and processes used in their manufacture, and to learn how to produce them with consistent, predictable, useful combinations of properties. The approach taken is microstructural, based on study and characterization of natural, commercial, and experimental carbons and graphites by such techniques as x-ray diffraction, electron and optical microscopy, and porosimetry. Physical and mechanical properties are measured as functions of formulation, treatment, and environmental variables, and correlations are sought among properties and structures. Raw material and manufacturing techniques are investigated, improved, and varied systematically in an effort to create specific internal structures believed to be responsible for desirable combinations of properties. Prompt feedback of information among these activities then makes possible progress in all of them toward their common goal of understanding and improving manufactured carbons and graphites.

Since its beginning, this program has been sponsored by the Division of Space Nuclear Systems of the United States Atomic Energy Commission, through the Space Nuclear Propulsion Office. More recently additional general support for it has been provided by the National Aeronautics and Space Administration, through the Office of Advanced Research and Technology. The direct and indirect support and the guidance and encouragement provided by both of these agencies of the United States Government are gratefully acknowledged.

II. CMF-13 "STATE-OF-THE-ART" GRAPHITE

Los Alamos Scientific Laboratory Report No. LA-3981, "The Manufacture and Properties of an Extruded, Resin-Bonded Graphite, CMF-13 Lot AAQ1", was issued on October 31, 1968. That report describes in detail the raw materials and manufacturing procedures used to produce Lot AAQ1, and lists its principal physical and mechanical properties, in most cases as functions of temperature. It has been distributed directly to all organizations and individuals who normally receive this Progress Report.

III. PUBLICATIONS RELATING TO CARBONS AND GRAPHITES

An appendix to this report lists the publications relating to carbons and graphites of which CMF-13 Staff Members are authors or coauthors. Several of these represent work done in cooperation with other LASL Groups, and a few report work done before the existing CMF-13 Graphite Research Group was organized.

This list will be kept up to date by noting in future Progress Reports each such publication as it is issued or appears in the literature.

IV. HIGHLY ORIENTED POLYCRYSTALLINE GRAPHITES

A. General

As part of the evaluation of several series of experimental grinding products, a large group of hot-molded graphites has been made in which these products were used as fillers. Several of the resulting graphites were quite unusual, and appeared potentially useful for a variety of applications. In particular, some of the fine, relatively flaky products of grinding natural graphite, pyrolytic graphite, and needle coke produced highly anisotropic graphites in which across-grain tensile strength and resistance to delamination seemed to be much higher than those of a pyrolytic graphite. In applications such as nose tips and heat shields for reentry vehicles, where a high degree of anisotropy can be used to advantage but delamination and spalling are disastrous, such a graphite may be valuable. It has the further advantages that it can be made by well-known techniques from common raw materials, is finely polycrystalline so that additives such as radiation absorbers and oxidation inhibitors can be finely disseminated in it, and its preferred orientation can probably be controlled to follow the contours of sharply curved and pointed bodies.

Because of current widespread interest particularly in reentry problems, a limited development program has been undertaken in which the production and properties of this class of materials will be explored in such depth as the group's manpower and equipment permit.

B. Characteristics and Property Requirements

For an application such as a reentry external heat shield, the principal requirements on the material used are: (1) Resistance to surface recession by sublimation, oxidation, and particle detachment; (2) Resistance to thermal shock and thermal stress; (3) Thermal conductivity through the material thickness sufficient to keep temperature and stress gradients at manageable levels, but not so high that heat transfer is excessive.

Except that it is subject to delamination and spalling, a properly oriented pyrolytic graphite should be outstandingly resistant to surface recession. Exposing only low-energy c-faces at the heated surfaces and with no binder-residue to offer paths for accelerated penetration from those surfaces, it should lose mass by sublimation and oxidation at a minimum rate. In an ordinary polycrystalline graphite, on the other hand, more active crystal planes are exposed more or less randomly at such a surface, and still more active binder-residues usually provide continuous paths for selective attack between filler particles. A highly oriented graphite made from a flaky, well-graphitized filler offers a possibility between these extremes. Most of the filler particles can be arranged to present c-faces at the surface, and overlapping of particles should block paths through binder residue at short intervals. (It may, in fact, be possible to find or develop a binder which graphitizes to produce a nearly homogeneous graphite, essentially eliminating these paths.) Such a material is not expected to equal a good pyrolytic graphite in resistance to surface recession, but may at least approach it.

The combination of more fundamental properties which leads to good thermal shock resistance is not well-understood. Clearly, however, high thermal conductivity parallel to the heated surface is desirable to remove heat from intensively heated regions, avoid hot spots, and reduce local shear stresses and the probability of local delamination, buckling, and spalling. At least in a heat shield, much lower conductivity is desirable normal to the surface, to reduce heat flow through the section. Unfortunately, low conductivity increases temperature gradients, thermal stress gradients, and the probability of thermal stress failure. Anisotropy of thermal conduction is evidently desirable, but it is not apparent what degree of anisotropy is optimum. Pyrolytic graphite is probably too highly anisotropic in this respect, and ordinary polycrystalline graphites not anisotropic enough. Flexibility in this regard is one of the most attractive features of the class of materials here considered.

Thermally developed stresses in a heat shield or nose tip are three-dimensional, so that pronounced anisotropy of strength properties is evidently undesirable. A major deficiency common to pyrolytic graphite and most laminated and filament-wound bodies is very low tensile strength normal to the layers composing the structure. It appears probable that highly oriented polycrystalline graphites can be developed which have a desirably high degree of anisotropy of thermal conductance, but much lower anisotropy of strength.

In general thermal stress is developed because thermal expansion of a surface layer is restrained by a cooler underlying layer. Compression is developed in the heated material, and balancing tension--which may lead to fracture--in material beneath it. A low thermal expansion coefficient parallel to the surface is desirable, to reduce the dimensional change which must be accomodated, and this is inherent in a highly oriented graphite. Low elastic modulus parallel to the surface is also desirable, to reduce the stress developed by a given dimensional change. This, unfortunately, is not typical of an oriented structure. However, an occasionally useful characteristic of a well-made polycrystalline graphite is that it contains fine, well-distributed voids. Particularly in compression, these are available to accomodate volume changes or shape changes of the graphite crystals, and the secant modulus in initial compressive loading drops rapidly below the tangent modulus measured at low load. In a porous body, then, the compressive stress developed by restraints on thermal expansion is reduced, and so is the balancing tension which restrains it. Low tensile elastic modulus and high strain to tensile fracture are also desirable, to reduce tensile stress developed by a given dimensional change and to postpone ultimate failure.

To the extent that these properties can be developed in a single material, that material should be useful in reentry and similar applications. A desirable combination of them appears possible in a highly oriented polycrystalline graphite, which it appears may combine good resistance to surface recession, good thermal shock properties, relatively low manufacturing cost, and a high degree of reproducibility.

C. Hot-Molded Anisotropic Graphites (R. J. Impreseia)

In the course of the grinding research described in the last previous report in this series (LA-3989-MS), a group of hot-molded, pitch-bonded graphites was produced in which the fillers were finely ground natural graphite, pyrolytic graphite, and needle coke. Some of the properties of those graphites are listed in that report (Table 5, page 9). Their densities ranged from about 1.63 to about 1.95 g/cm^3, and their crystalline anisotropies from M = 2.8 to M = 10.2. They were manufactured as disks only 5/8 to 3/4 in. thick, so that their across-grain mechanical properties could not be determined by standard tests.

Principally to permit machining of full-size test pieces for physical and mechanical testing, a group of generally similar graphites has since been made in the form of cylinders 2.5 to 4 in. dia and 2.3 to 2.7 in. high. The raw materials used are listed in Table I, the mix formulations and molding conditions in Table II, and the properties so far determined in Table III.

TABLE I

RAW MATERIALS USED TO MANUFACTURE HOT-MOLDED ANISOTROPIC GRAPHITES

Material Identification	Material Description
GP(Py)-3	Ground pyrolytic graphite
GP(Py)-10	Ground pyrolytic graphite
G(Na)-21	Natural graphite flakes (Southwestern Graphite Co. Grade 1651)
CN-3	Needle coke flour (Carbon Products Division, Union Carbide Corporation)
G-20	Graphite flour (Carbon Products Div., Union Carbide Corp., Grade GP38)
TP-4	Thermax carbon black (Thermatomic Carbon Co.)
Varcum	Furfuryl alcohol resin (Uncatalyzed, Reichold Chemical Co. Grade 8251)
Pitch	Barrett 30 MH pitch (Allied Chemical Co.)

TABLE II

MIX FORMULATIONS AND MOLDING CONDITIONS, HOT-MOLDED ANISOTROPIC GRAPHITES

Specimen No.	Mix Composition, Parts by Weight		Molding Conditions		% Change, Baked to Graph.	
	Filler	Binder	Pressure psi	Temp °C	Δl	Δd
49 B-2	80 GP(Py)-3 + 20 TP-4	40 Vacuum	2000	900	-2.3	-0.04
50 B-1	80 G(Na)-21 + 20 TP-4	20 Pitch	1500	900	-1.4	-0.3
50 D-1	100 G(Na)-21	30 Vacuum	1000	900	+0.3	-0.3
50 E-1	100 GP(Py)-10	20 Pitch	1500	900	-4.0	+2.5
50 F-1	100 GP(Py)-10	20 Pitch	1000	720	-3.3	+1.9
50 G-1	100 GP(Py)-10	30 Pitch	1000	700	-1.3	+1.0
50 H-1	80 GP(Py)-10 + 20 G-20	30 Pitch	1000	900	-2.8	+1.8
50 I-1	80 GP(Py)-10 + 20 CN-3	30 Pitch	1000	870	-1.3	+0.9
50 K-1	100 GP(Py)-10	26 Vacuum	1000	700	---	---
50 P-1	80 GP(Py)-10 + 20 G-20	30 Pitch	2000	900	-0.9	+1.1
50 Q-1	80 GP(Py)-10 + 20 CN-3	30 Pitch	2000	900	-1.6	+0.9
50 R-1	80 GP(Py)-10 + 20 G(Na)-21	26 Vacuum	4000	900	+0.8	+0.7
50 S-1	80 GP(Py)-10 + 20 G(Na)-21	26 Vacuum	1000	880	-0.8	+0.7
50 T-1	80 GP(Py)-10 + 20 G(Na)-21	30 Pitch	1000	900	-1.7	+1.1

Because of equipment limitations, molding pressures were generally much lower than those used in producing the previous series of smaller disks, and bulk densities were correspondingly low. Pitch-bonded specimens were hot-molded using a constant heating rate of 15°/min to 900°C, with a 1-hr hold at 900°C. Resin-bonded specimens were heated to 900°C in an 8.5-hr cycle which involved slow heating through temperature regions in which large exotherms were known to occur. Because of equipment difficulties, not all runs reached 900°C. All specimens were therefore baked in vacuum at 900°C, and then graphitized in flowing helium to 2700°C or higher.

Presumably because their porosities were undesirably high, some of the properties of these graphites were disappointingly low. However, with-grain thermal conductivities were relatively high, and anisotropy of thermal conduction was indeed distinctly higher than anisotropy of tensile strength. In spite of low density, Specimen 50 B-1 showed useful tensile strength in both orientations. With-grain thermal expansion coefficients were generally low, dynamic Young's moduli moderate, and strain to fracture in a few cases relatively high.

Thermal shock indices, however formulated, are at best only a qualitative indication of resistance to thermal shock and thermal stress. They are convenient, however, for preliminary comparisons among generally similar materials. Those listed in Table III for with-grain orientations are quite high, and are of the magnitude expected for a good, molded, commercial graphite such as ATJ. Those listed for across-grain orientations are extremely low, relative even to across-grain indices for highly oriented commercial graphites such as hot-worked ZTA. They should, however, probably be compared with the across-grain value for a pyrolytic graphite, which is about 0.06. The materials listed in Table III should, on this basis, have thermal shock resistance normal to an external surface from about 80 to about 200 times that of a good pyrolytic graphite.

These materials are believed to have sufficient promise to justify further development, and perhaps eventual direct testing of their thermal shock and ablation behavior.

TABLE III

PROPERTIES OF HOT-MOLDED ANISOTROPIC GRAPHITES

	Specimen No. [a]							
	49 B-2		50 B-1		50 D-1		50 I-1	
	WG	AG	WG	AG	WG	AG	WG	AG
Bulk Density, g/cm^3, Baked	1.699		1.661		1.722		1.668	
Bulk Density, g/cm^3, Graphitized	1.703		1.648		1.673		1.649	
Young's Modulus, 10^6 psi	1.237	0.283	2.893	2.003	1.429	0.614	---	---
Shear Modulus, 10^6 psi	---	0.202	0.662	0.422	0.699	---	0.247	0.185
Internal Friction, $x10^{-3}$ tan α	6.9	14.9	6.9	8.6	5.4	10.8	---	---
Tensile Ultimate Strength, psi	---	328	2541	1556	1819	735	1606	344
Tensile Yield Strength, 0.2%, psi	---	279	---	---	---	639	---	209
Tensile Strain to Fracture, %	---	0.23	0.20	---	0.14	0.12	0.37	0.30
Compressive Ultimate Strength, psi	3398[c]	2807	4809	7096	3821	4044	2937	3748
Compressive Strain to Fracture, %	0.15	0.41	2.4	---	0.20	1.5	0.15	---
Thermal Exp. Coeff., $x10^{-6}$/°C[b]	0.81	7.65	1.18	9.32	1.16	8.03	0.91	8.18
Thermal Conductivity, W/cm-°C	0.73	0.240	1.273	0.246	1.217	0.388	1.187	0.165
Electrical Resistivity, $\mu\Omega$cm	1913	11,017	877	5387	986	3368	1530	18,730
Anisotropy Ratios:								
Young's Modulus	4.4		1.4		2.3		---	
Shear Modulus	---		1.6		---		1.3	
Internal Friction	2.2		1.2		2.0		---	
Tensile Ultimate Strength	---		1.6		2.5		4.7	
Tensile Strain to Fracture	---		---		1.2		1.2	
Compressive Ult. Strength	---		1.5		1.1		1.3	
Compressive Strain to Fracture	2.7		---		7.5		---	
Thermal Exp. Coeff.	9.4		7.9		6.9		9.0	
Thermal Conductivity	3.0		5.2		3.1		7.2	
Electrical Resistivity	5.8		6.1		3.4		12.2	
Thermal Shock Index[d]	---	9	226	5	319	14	---	---

(a) WG = with-grain, AG = across-grain

(b) Average 25-645°C except 25°-500°C for No. 49 B-2

(c) Orientation may be incorrect

(d) $kS/\alpha E$, with all units as above except that k has been converted to cal/cm-sec-°C

TABLE IV

CHARACTERIZATION OF HCTE GRAPHITE FLOURS

Sample	Helium Density g/cm³	Micromerograph Sample Statistics (a) $\hat{\mu}_{x3}$	$\hat{\sigma}_x^2$	$\hat{\mu}_x$	$\bar{d}_3$	$\bar{d}$	s_d^2	S_W, cm²/g
G-23	2.12	4.233	1.172	0.7159	123.8	3.677	30.14	738
G-24	2.13	3.009	0.6458	1.071	27.93	4.032	14.76	1920
G-25	2.13	4.165	1.753	-1.093	154.7	0.805	3.09	1055

(a) Calculation based on log-normal model

V. RAW MATERIALS

A. Solid Raw Materials (H. D. Lewis)

1. Characterization of HCTE Graphite Flours

Three lots of HCTE (high coefficient of thermal expansion) graphite flour, identified as CMF-13 Lots G-23, G-24 and G-25, have been characterized with regard to helium density and particle size distribution. Results are listed in Table IV. These are "secondary" graphite flours produced by Carbon Products Division of Union Carbide Corporation by grinding a graphite made from an air-blown HCTE coke ("Robinson Coke") and coal-tar pitch. They are being used in CMF-13 to produce a series of experimental extruded graphites intended to be nearly isotropic and to have high expansion coefficients.

2. Surface-Area Analyses

Surface-area analyses have been made by the BET (nitrogen-adsorption) method on coarse (FA), medium (FB), and fine (FC) fractions of ground commercial grade YBF graphite, and on the products of grinding these further at various feed rates in a Trost fluid-energy mill. Results will be reported in connection with grindability studies, described below.

3. Mixture Calculations

The FININT computer program has been used to calculate mixture statistics for several systems composed of G-25 graphite flour (an HCTE flour described above), G-18 graphite flour (Great Lakes 1008 graphite flour), and the +38μ, -38μ, +53μ, and -53μ fractions of the G-18 flour. These calculations were used to construct diagrams predicting relative density as a function of mixture composition for various binary combinations of these flours. Extruded graphites are now being manufactured to compare predicted and observed relative densities for each system.

B. Liquid Raw Materials (E. M. Wewerka)

1. Furfuryl Alcohol Resins

An attempt is being made to identify the low-molecular-weight species in furfuryl alcohol resins by separating them by vacuum distillation followed by gas chromatography, and identifying them by infrared spectroscopy, mass spectrometry, and elemental analysis. Elemental analyses have been completed on several samples collected from the gas chromatograph, and in general correlate well with preliminary infrared identifications.

The effects of viscosities of acid-catalyzed furfuryl alcohol resin binders on the properties of extruded graphites made from them are now well documented. Two series of acid-catalyzed resins designed to investigate the effects of molecular distribution have been synthesized, and are being used as binders in the manufacture of experimental graphites. A series of resins catalyzed with γ-alumina is now being synthesized to determine the effects of viscosity of binders of this type, and to permit a direct comparison of graphites made from them with graphites made from comparable acid-catalyzed resins.

2. Furfuryl Alcohol-Formaldehyde Copolymers

Evaluation of furfuryl alcohol-formaldehyde colymers as binders for graphite is continuing. Three additional series of resins have been prepared and are now being tested, including a reference series of standard furfuryl alcohol resins, copolymers having a 10:1 ratio of furfuryl alcohol to formaldehyde, and copolymers having a 2:1 ratio of furfuryl alcohol to formaldehyde. In general, several members of each series are carbonized in the absence of any filler, used as binders with a standard filler to produce extruded rods, and used as binders with a filler having large crystallite size to produce molded compacts. Information is collected on carbon residue, degree of graphitization, and such properties as density and strength.

To this point, none of the copolymers investigated appears particularly promising for use as a binder. However, additional resins and further evaluations are required before a decision on the usefulness of this type of copolymer can be made.

3. Donor-Acceptor Complexes

The study of donor-acceptor complexes of vinyl ethers and tetracyanoethylene (TCNE), directed toward possible initiation of polymerization reactions by charge-transfer mechanisms, has continued. It now seems clear that many problems previously attributed to component instability were actually due to formation of donor-acceptor complexes between TCNE and the solvents used. These complicated the interpretation of TCNE band positions and the identification of TCNE-vinyl ether charge-transfer bands. Acetonitrile, however, appears to complex very little with TCNE, and will hereafter be used generally as a solvent for these systems.

The charge-transfer bands of TCNE and butyl vinyl ether (BVE) and of tetracyanoquinodimethane and BVE in acetonitrile have been identified in the ultraviolet-visible region. At the concentrations required to follow simultaneously the changes of the bands of the acceptor and donor molecules, equilibrium in these two systems is approached very slowly. Further work at higher component concentrations will be attempted.

At low concentration ($\sim 10^{-5}$M), no evidence of donor acceptor complex formation could be detected in the TCNE-BVE system in methylene chloride. However, the large charge-transfer band between TCNE and the solvent may have obscured a TCNE-BVE charge-transfer band.

4. Resins for Carbon Foams

In collaboration with LASL Group CMB-6, a limited investigation has been undertaken of resins potentially useful for the manufacture of carbon foams. Eight experimental resins (EMW No. 155, 171, 185, 205, 206, 207, 208 and 212) have been synthesized and furnished to Group CMB-6, who will investigate their foaming behavior and the properties of the foams produced. These include standard furfuryl alcohol resins, 10:1 furfuryl alcohol-formaldehyde copolymers, and 2:1 furfuryl alcohol-formaldehyde copolymers, each at several different viscosities. A sample of a commercial alumina polymerized furfuryl alcohol resin (Karbo 44/L) has also been provided. A new urethane foam formulation is being tested for compatability with these resins.

The urethane formulation currently used utilizes a reaction between a diisocyanate and a polyfunctional hydroxyl compound:

$$HO\text{-}R'\text{-}OH + OCNRNCO \rightarrow (-R'\text{-}O\text{-}\overset{O}{\overset{\|}{C}}\text{-}NH\text{-}R\text{-}NH\text{-}\overset{O}{\overset{\|}{C}}\text{-}O)_n .$$

(In addition to the main reactants, catalysts, emulsifiers and surfactants are usually added to the system.) The urethane foam is apparently intended to act only as a carrier for the resin, which is the principal source of carbon, and not to react with it. However, in the case of furfuryl alcohol resins, the possibility exists that monofunctional hydroxyl groups in these resins will react with diisocyanate groups from the urethane to prevent reaction to higher polymers. This would leave a system of low molecular weight polymers with undesirable foaming properties. To avoid this difficulty, the most promising approach appears to be an effort to eliminate the free hydroxyl groups from the furfuryl alcohol resins, or alternatively to compensate for them as much as possible. This can be accomplished in a number of ways, including:

(a) Polymerization of acid-catalyzed furfuryl alcohol

resins to the highest degree compatible with subsequent processing.

(b) Use of resins of low inherent hydroxyl content, such as the alumina-polymerized resin mentioned above.

(c) Inclusion in the urethane formulation of additional diisocyanate molecules to compensate for the hydroxyl groups present in the resin.

VI. EXPERIMENTAL GRAPHITE MANUFACTURE

A. Grinding Research (R. J. Impresoia)

As was reported in LA-3032-MS, an investigation has been undertaken of the effect of mill variables on the rate at which a given material is reduced in a Trost fluid-energy grinding mill. For the first experiments in this investigation, a coarsely ground commercial YBF graphite -- from lot GP(YBF)-6 -- was separated into three size fractions by repeated screening on a SWECO Vibro Energy Separator. These were a coarse (-34+62 mesh) fraction used for grinding series FA, an intermediate (-62+100 mesh) fraction used for series FB, and a fine (-100+200 mesh) fraction for series FC. Samples of each fraction were ground in the Trost mill using a variety of feed rates, and each grinding product was characterized with regard to relative fineness (wt % $<10\mu$) and specific surface area measured both by the BET (nitrogen-adsorption) method and by the permeability method (using a Fisher Sub-Sieve Sizer). Data for the FB series are summarized in Table V, together with calculated grindabilities.

Grindability, P, is defined as the rate of change during grinding of some particle characteristic which represents energy absorbed, relative fineness, etc. In Table V, three different grindability indices are shown, one based on change in surface area measured by nitrogen adsorption, one on change in surface area measured by gas permeability, and one increase in weight fraction of particles finer than 10μ, measured by micromesh sieving. In each case the change has been multiplied by the feed rate to the mill, so that grindability is expressed as total increase in surface area or weight of fines per minute.

At the lower feed rates, increase in surface area per gram and in proportion of fines was large, as might be expected from the fact that a large amount of energy was available to a relatively small number of particles. However, grindability -- representing total new surface or weight of fines produced per unit time -- was low, because of the low rate at which material was passed through the mill. With increasing feed rate the amount of new surface or of fines produced per gram of material passing through the mill was reduced, but grindability increased. As is shown in Fig. 1, the increase was at first approximately linear with feed rate. At about 10 g/min a maximum was reached after which grindability decreased, as

TABLE V

SPECIFIC SURFACE AREA, FINENESS, AND GRINDABILITY AS FUNCTIONS OF FEED RATE; INTERMEDIATE FRACTION, YBF GRAPHITE

Grind No.	Feed Rate R g/min	BET SURFACE S_B m^2/g	BET SURFACE $S_B - S_{Bo}$ m^2/g	BET SURFACE P_B m^2/min	PERM SURFACE S_P m^2/g	PERM SURFACE $S_P - S_{Po}$ m^2/g	PERM SURFACE P_P m^2/min	FINES F % $<10\mu$	FINES P_F $g<10\mu/min$
FB-Feed	---	2.14(S_{Bo})	---	---	0.05(S_{Po})	---	---	0	---
FB-1	1.8	13.40	11.26	20.3	2.61	2.56	4.62	91.9	1.7
FB-2	3.8	13.02	10.88	41.3	2.30	2.25	8.56	77.2	2.9
FB-3	8.5	10.32	8.18	69.5	1.81	1.76	15.02	58.5	5.0
FB-4	18.5	5.55	3.41	58.1	0.75	0.70	12.91	23.0	4.3
FB-5	31.0	4.65	2.51	77.8	0.51	0.46	14.29	17.4	5.4
FB-6	69.8	3.75	1.61	112.4	0.31	0.26	18.63	10.2	7.2

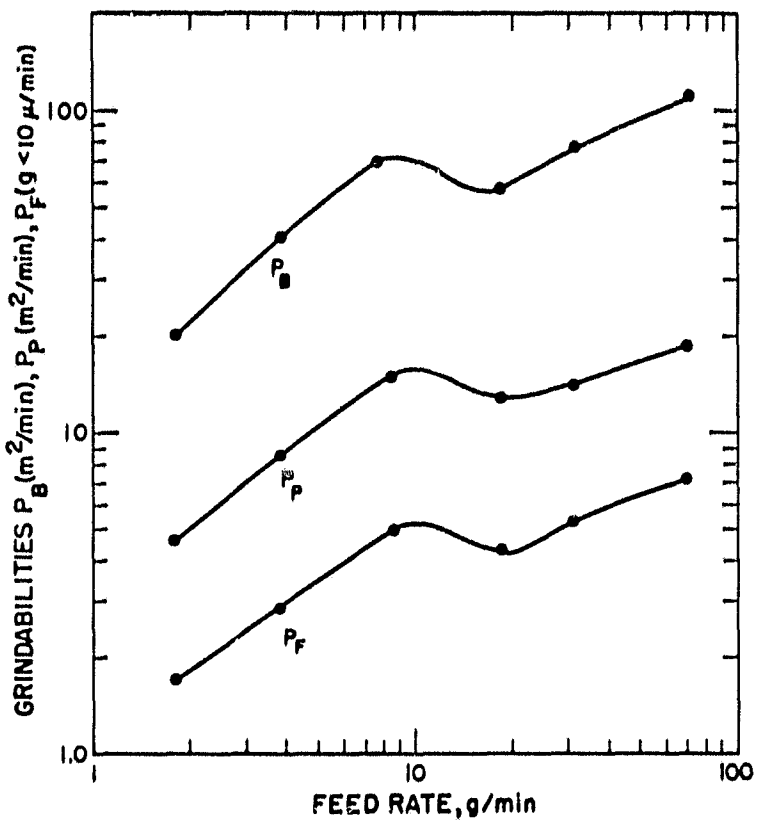

Fig. 1. Grindabilities of FB graphite as functions of feed rate to Trost fluid-energy mill.

would be expected if the mill became overloaded. Unexpectedly, however, grindability again increased with feed rate when rates were above about 20 g/min, and continued to do so to about 70 g/min, where the mill became choked (as was indicated by severe blowing back of feed material).

At low feed rates the grinding action in this mill is apparently "first-order". Grindability is linear with feed-rate, by particle-on-particle impact. The maximum in the grindability curve probably appears at the point at which the concentration of particles in the mill has become great enough so that particles in the same stream interfere with each other, reducing the momentum per particle attained before they impinge on the opposing stream of particles. The subsequent increase in grindability at high feed rates must represent some change in grinding mechanism. This may be an increase in mutual attrition within the particle stream, occurring when particle crowding is severe. This would be favored by the fact that, with less reduction in size per particle, average particle size within the mill becomes larger, and larger particles in general are weaker than small ones produced from them.

Since the three curves of Fig. 1 are approximately parallel, it appears that -- at least for this material -- any of the three grindability indices used is a useful indication of grinding behavior.

B. Mixing Experiments (R. J. Impreseia)

In the hope of developing a nearly isotropic, low-permeability graphite made from commercially available materials, a group of six commercial fillers was selected for initial mixing experiments. The group included three relatively coarse flours (Lots C-1, C-10 and G-14) and three finer ones (Lots C-3, C-8 and G-24). Four, identified by the letter C, were coke flours and two, identified by the letter G, were graphite flours.

Eight binary combinations of these flours, each including a coarse and a finer component, have been investigated. The weighed fillers for each mix were blended together for 10 min in a Fisher-Kendall laboratory bottle blender. Then an amount of stearic acid representing slightly less than the optimum binder concentration was added, and blending was continued for 10 min. The mix was compacted in a 1.5-in. dia steel die at 900 psi, and the dimensions of the ejected compact were measured. From the known weight of filler and the volume of the compacted mixture, a packed filler density was calculated. Both the blending procedure and the compacting pressure were selected to minimize the probability of filler-particle fragmentation.

Packed filler density as a function of mix composition is plotted for each binary system in Fig. 2 through 9. In six of the eight systems there is an intermediate composition at which the filler mix compacts to higher density than does either of the pure components. In one system, Series 41 shown in Fig. 2, there is a small peak in the density curve, but at a value no higher than that of one of the components. Series 42 (Fig. 3) shows no maximum. Series 47 (Fig. 8) is unusual in showing two separated maxima. In each plot, each extreme point and each point in the vicinity of a maximum represents the average of at

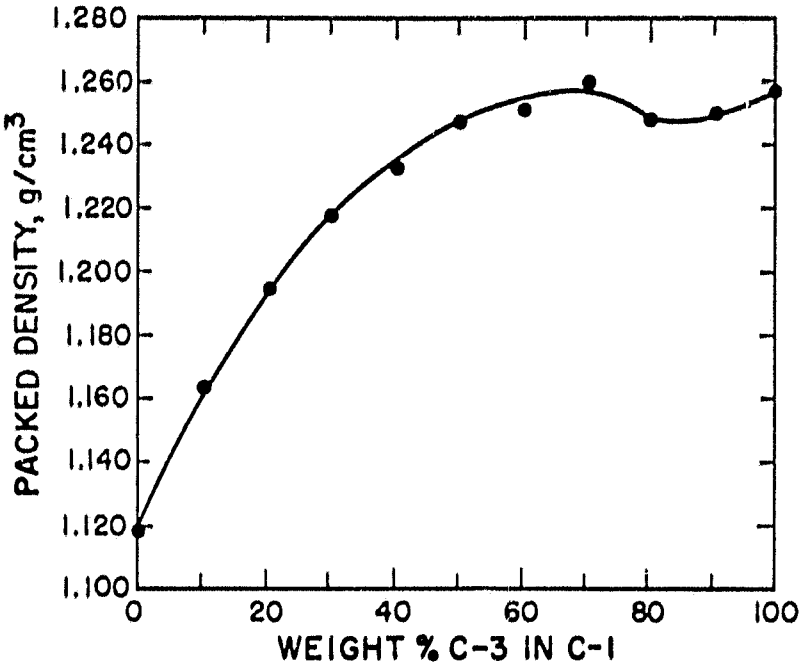

Fig. 2. Packed filler density vs. composition, Series 41.

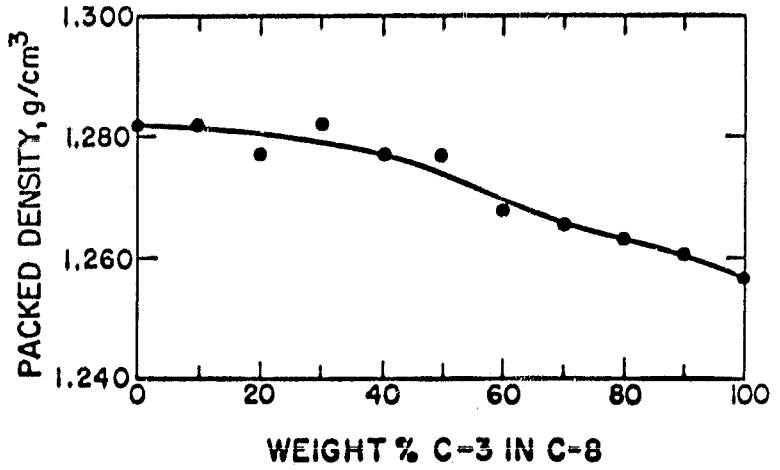

Fig. 3. Packed filler density vs. composition, Series 42.

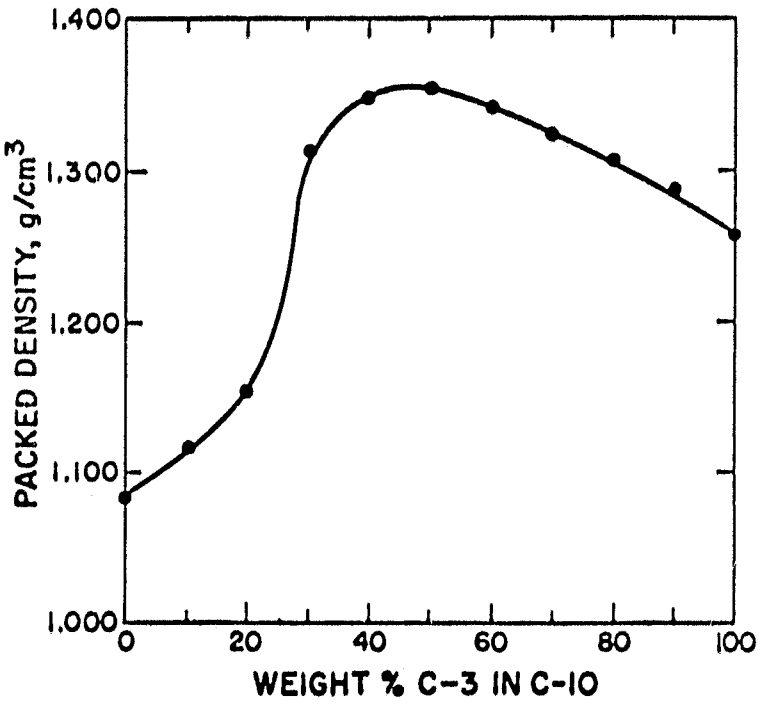

Fig. 4. Packed filler density vs. composition, Series 43.

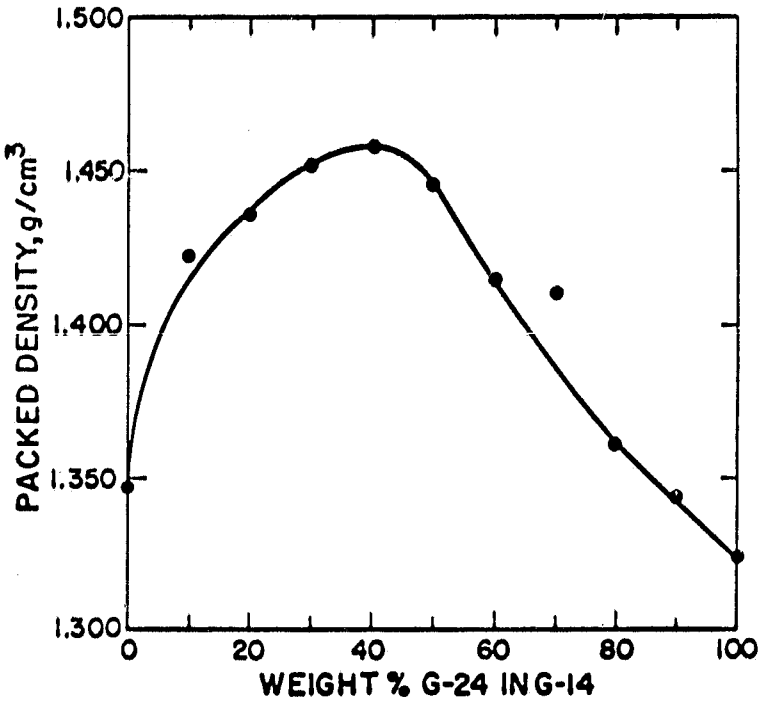

Fig. 5. Packed filler density vs. composition, Series 44.

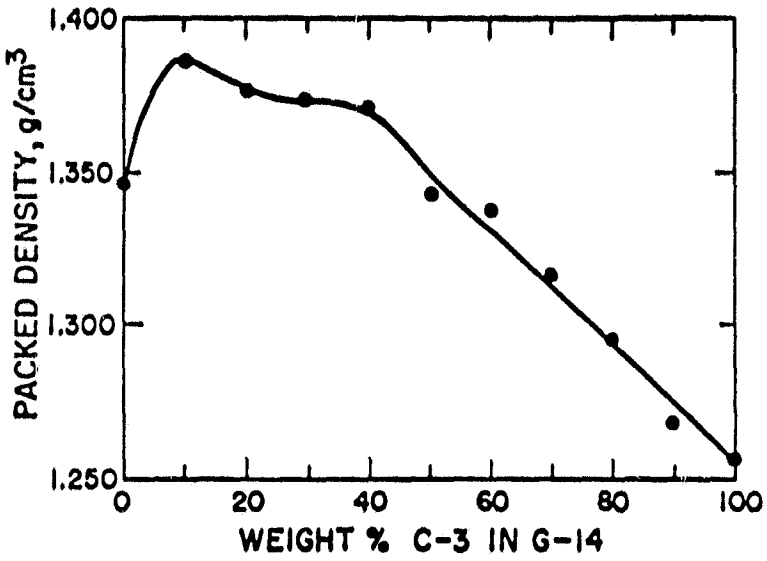

Fig. 6. Packed filler density vs. composition, Series 45.

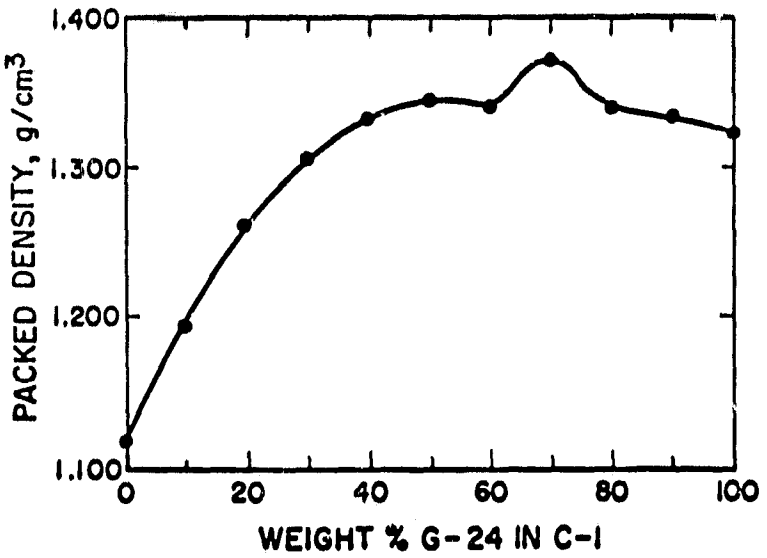

Fig. 7. Packed Filler density vs. composition, Series 46.

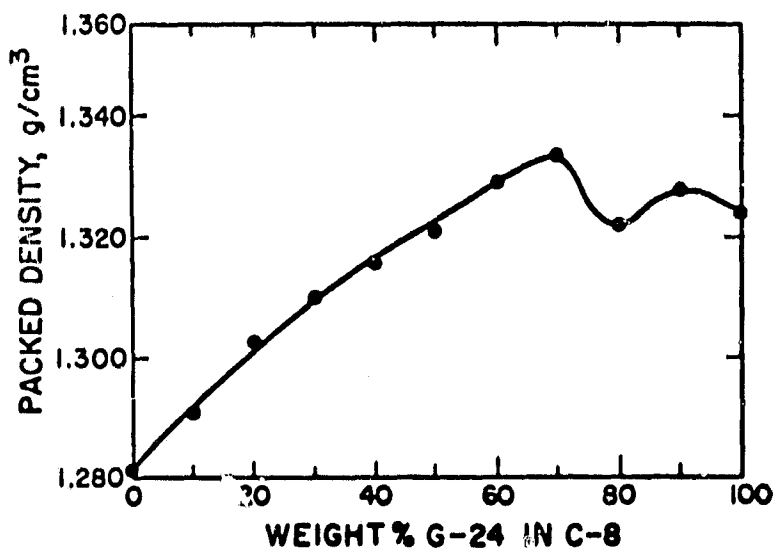

Fig. 8. Packed filler density vs. composition, Series 47.

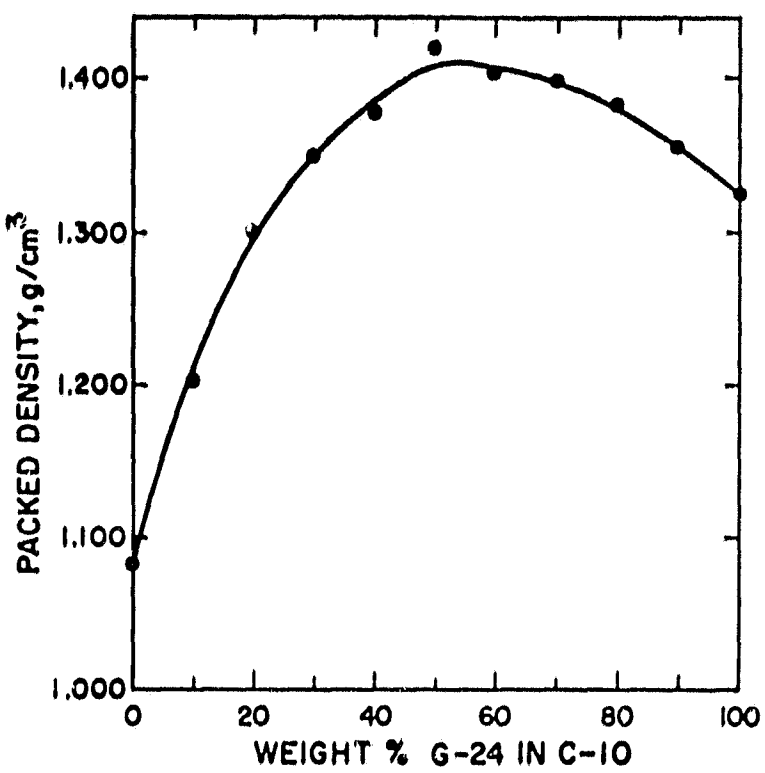

Fig. 9. Packed filler density vs. composition, Series 48.

least two independent determinations. Each point in the region of the double peak in Fig. 8 is the average of three determinations.

For each system in which a maximum occurred at a density higher than that of either component, the composition which produced maximum density was identified and assigned a "mix number", which is listed in Table VI. Each of these mixes was used as the basis of a further series of similar experiments in which the effect on packed filler density of additions of Thermax carbon black (Lot TP-3) was investigated.

Mixtures of Thermax with the binary filler mix were prepared and molded as described above. Packed filler densities for each ternary series are plotted as functions of Thermax content in Fig. 10 through Fig. 15. With the exception of the extreme points on each curve, which are average values from at least two determinations, each point represents one determination only. In only one case (Fig. 10, Thermax added to Mix No. 1) did the carbon black addition produce a further increase in packed density of the binary filler mix, and even here the increase was small. Evidently, even at low concentrations, the Thermax particles do not just enter voids in the structure, but also occupy positions between filler particles

TABLE VI

BINARY MIX COMPOSITIONS WHICH PRODUCED MAXIMUM PACKED FILLER DENSITY

Mix No.	Mix Composition, Parts by Weight Component A	Component B	Packed Filler Density, g/cm^3	Series No.
1	55 parts C-10	45 parts C-3	1.35	43
2	60 parts G-14	40 parts G-24	1.46	44
3	90 parts G-14	10 parts C-3	1.39	45
4	30 parts C-1	70 parts G-24	1.37	46
5	30 parts C-8	70 parts G-24	1.33	47
6	50 parts C-10	50 parts G-24	1.42	48

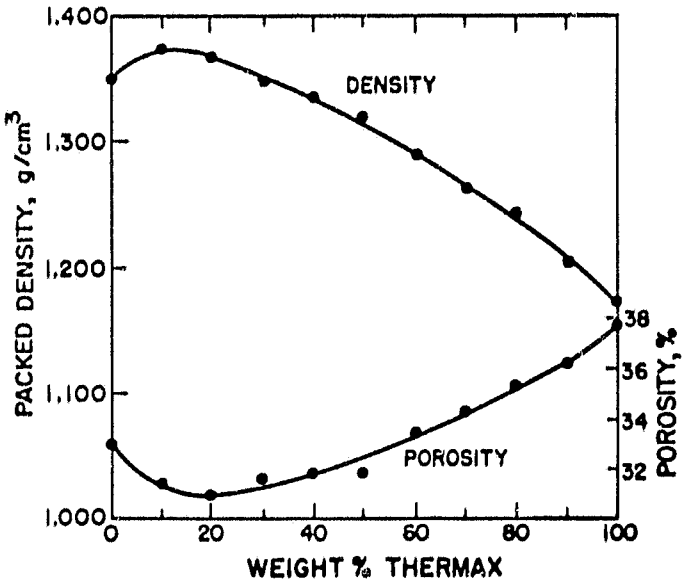

Fig. 10. Packed filler density and porosity vs. composition, Mix No. 1 plus Thermax.

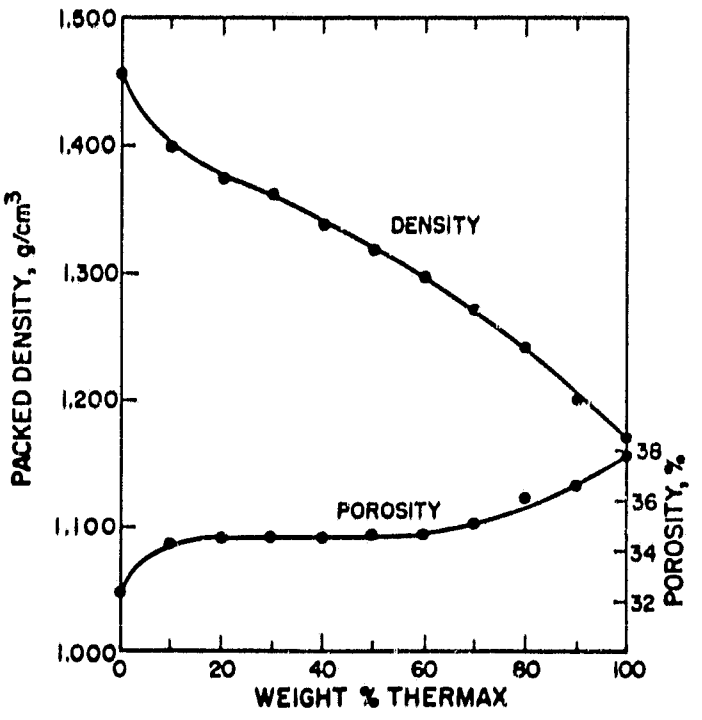

Fig. 11. Packed filler density and porosity vs. composition, Mix No. 2 plus Thermax.

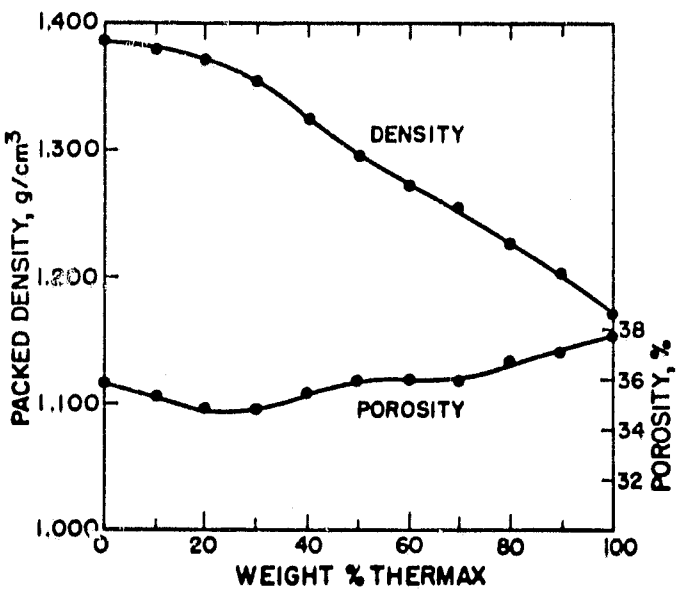

Fig. 12. Packed filler density and porosity vs. composition, Mix No. 3 plus Thermax.

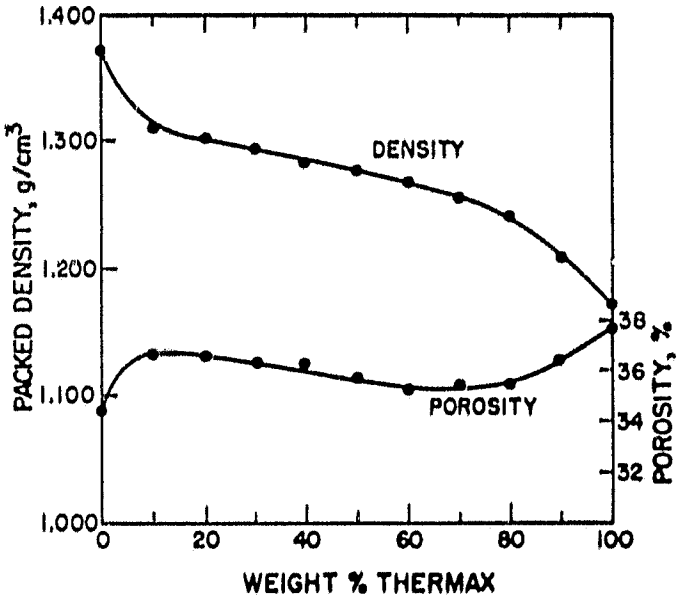

Fig. 13. Packed filler density and porosity vs. composition, Mix No. 4 plus Thermax

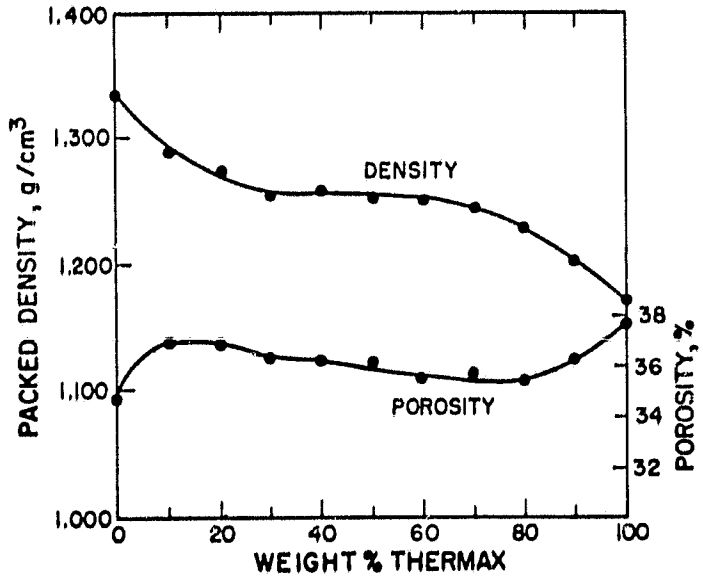

Fig. 14. Packed filler density and porosity vs. composition, Mix No. 5 plus Thermax.

and expand a network which is initially quite closely packed. The particle density of Thermax (1.88 g/cm^3) is significantly lower than those of the other components of these mixes (2.0 to 2.2 g/cm^3). Therefore the mass contributed by the carbon black addition is not sufficient to compensate for the expansion it produces, and in general in these systems density decreases when it is added.

The effect of Thermax on compaction behavior is perhaps more clearly shown by plotting porosity as a

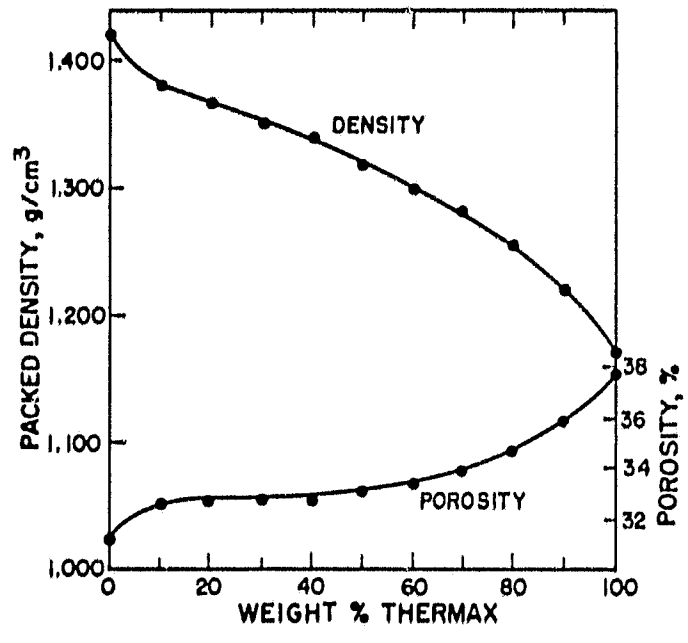

Fig. 15. Packed filler density and porosity vs. composition, Mix No. 6 plus Thermax.

function of Thermax content, as has also been done in Fig. 10 through 15. The volume occupied by each mix component (including internal voids which are not surface connected) was calculated from its weight and particle density, the latter measured in a helium pycnometer. The fraction of specimen volume not occupied by particles was identified simply as "porosity", although obviously it does not include enclosed voids within filler particles. From this set of curves it is evident that minimum porosity does not necessarily coincide with maximum packed filler density. Thus, in Fig. 10, the density maximum is at about 10% Thermax, and the porosity minimum is at about 20%. In Fig. 12 there is no density maximum, but a porosity minimum appears at about 25% Thermax. In Fig. 14 porosity diminishes while density remains nearly constant, and in Fig. 11 and 15 porosity remains nearly constant while density is decreasing quite rapidly. Obviously, in some systems, porosity and density can be adjusted almost independently of each other.

Pitch-bonded specimens, molded at 4000 psi and 900°C, have been made from the filler mixes which produced maximum densities and minimum porosities in the six systems shown in Fig. 10 through 15. In the two cases where maximum density and minimum porosity do

TABLE VII

POROSITIES AND DENSITIES OF HOT-MOLDED GRAPHITES

Specimen No.	Filler Components: Mix No.	Filler Components: Thermax %	Calculated Porosity, %[d]: Packed Filler	Calculated Porosity, %[d]: Bulk Specimen	Density, g/cm^3[e]: Packed Filler	Density, g/cm^3[e]: Bulk Specimen	Graphitized[f] Bulk Density g/cm^3
43E-2	1	10[b]	24.5	16.8	1.511	1.664	1.657
43F-1	1	20[c]	24.6	16.7	1.501	1.657	1.660
44E-1	2	0	21.9	16.0	1.686	1.815	1.780
45E-1	3	0	23.7	16.8	1.648	1.798	1.664
45F-1	3	25[c]	20.4	13.9	1.663	1.799	1.774
46E-1	4	0	26.6	18.7	1.534	1.699	1.710
47E-1	5	0	27.0	18.3	1.533	1.715	1.742
48E-1[a]	6	0	25.2	18.4	1.541	1.681	1.669

(a) Numerous surface cracks; properties probably not reliable.

(b) Composition selected to give maximum density.

(c) Composition selected to give minimum porosity.

(d) As hot-molded. Does not include enclosed porosity within filler particles.

(e) As hot-molded.

(f) Graphitized at 2800°C.

not coincide (Fig. 10 and 12), mixes were used of both compositions. Results are listed in Table VII. Because of the presence of the pitch-binder residue, calculated porosities are lower and densities higher for the bulk specimens than for the packed fillers. Data for the bulk specimens, including bulk density after graphitization, are not relevant to the packing investigation being considered here, but are of practical interest with regard to the graphites that may evolve from this study.

Although the curve of Fig. 10 predicts lower porosity for Specimen 43 F-1 (20% Thermax) than for Specimen 43 E-2 (10% Thermax) in fact the two specimens were nearly identical in this regard. This may be because the pressure used in hot-molding, which was more than four times that used in the experiments leading to Fig. 10, was sufficient to crush some filler particles and improve packing. Specimen 45 F-1, containing 25% Thermax in the filler and expected to have minimum porosity, indeed had 3.3% less interparticle porosity than did Specimen 45 E-1, which contained no Thermax. However, density was also increased by the Thermax addition, which would not be predicted from Fig. 12. This again may be an effect of higher molding pressure. Specimens 44 E-1 and 45 F-1 show the lowest interparticle porosities and highest packed filler-particle densities of any graphites in this series, and so are interesting for further development.

C. Extrusion Variables (J. M. Dickinson)

Many factors affect the properties of extruded graphites, including the variables of the extrusion process itself. The more important extrusion variables are die-system design, speed, pressure, vacuum and temperature. Binder-to-filler ratio in the mix being extruded, effectiveness of blending and conditioning treatments, etc, are also important beyond their direct effects on structure because they affect most of the extrusion parameters.

In order to evaluate the interplay among these many variables, the CMF-13 extrusion press has recently been instrumented to monitor the principal extrusion conditions continuously. In the meantime several series of experi-

TABLE VIII

EXTRUSION CONDITIONS AND PROPERTIES, ABE GRAPHITES

Specimen No.	Die Used	Extrusion Conditions: Pressure psi	Extrusion Conditions: Speed in./min	Extrusion Conditions: Temp. °C	Green Rod Dia. in.	Graphitized Properties: Rod Dia. in.	Graphitized Properties: Density g/cm^3	Graphitized Properties: Electr. Resist.[a] μΩcm	Graphitized Properties: Young's Modulus[a] 10^6 psi	Graphitized Properties: Compr. Strength psi	Graphitized Properties: Crystalline Anisotropy[a] M	Graphitized Properties: Crystalline Anisotropy[a] σ_{ox}/σ_{oz}
ABE1	Normal	6400	171	46	0.5005	0.4757	1.885	967	2.54	8760	2.1	1.45
ABE2	Short-land	6400	124	42	0.508	0.5056	1.891	1072	2.35	8369	1.5	1.35

(a) With-grain properties.

ments have been conducted to examine individually some of the more important variables.

1. Die Design (Series ABE)

The ABE series of graphites was made to examine the effects of shortening the land of a "standard" extrusion die by a factor of four, from 2 in. to 0.5 in., with all other variables kept as nearly constant as possible. The mix contained 85 parts G-18 graphite flour, 15 parts TP-4 Thermax carbon black, and 27 parts Varcum furfuryl alcohol resin, and was extruded through 0.500-in. dia dies. The extruded rods were cured and baked using cams 12 and 16 (described in LA-3989-MS, page 23) and graphitized to 2830°C. Extrusion conditions and properties of these graphites are summarized in Table VIII. All rods appeared to be sound and of high quality.

Although extrusion pressure was the same for the two lots of graphite, extrusion temperature was slightly higher and extrusion speed much higher when the normal die (Die No. 1) was used. With the short-land die (Die No. 2), diameter of the green rod was much greater and it subsequently shrank less during graphitizing. It also had far higher density than has previously been observed for rods which expanded appreciably as they left the die. Preferred orientation was considerably reduced by shortening the die land, which may account for the differences in with-grain electrical resistivity, Young's modulus, and compressive strength. No microscopic evidence was found of an internal crack system or any other microstructural feature associated with expansion of the green rod as it left the die.

Unfortunately, linear shrinkage and carbon residue were not measured in this experiment. It will be repeated, with additional measurements, in part simply to confirm the very important observation that a relatively large change in anisotropy can be produced by a very simple change in die design.

2. Binder Content (Series ABD)

Small variations in green diameter and final density of resin-bonded graphites made under nearly the same conditions have often been observed, and usually no reason for them has been apparent. One possible reason is small variations in initial binder content. Another is evaporative loss of part of the binder prior to extrusion.

To investigate the effects of relatively small variations in binder content, four extruded graphites were made under very carefully controlled conditions using 25 to 28 parts of Varcum binder to 85 parts G-18 graphite flour and 15 parts TP-4 Thermax carbon black. In all cases time between mixing and extrusion was minimized. Results are plotted in Fig. 16, with pore "size" statistics derived from mercury porosimetry listed in Table IX. Green diameter is a minimum at 27 pph of binder, the binder level believed from previous work to be the optimum. Electrical resistivity is also a minimum at this value, as is average pore "size" indicated by $\bar{X}_3$. Both density and Young's modulus have maxima at this same binder

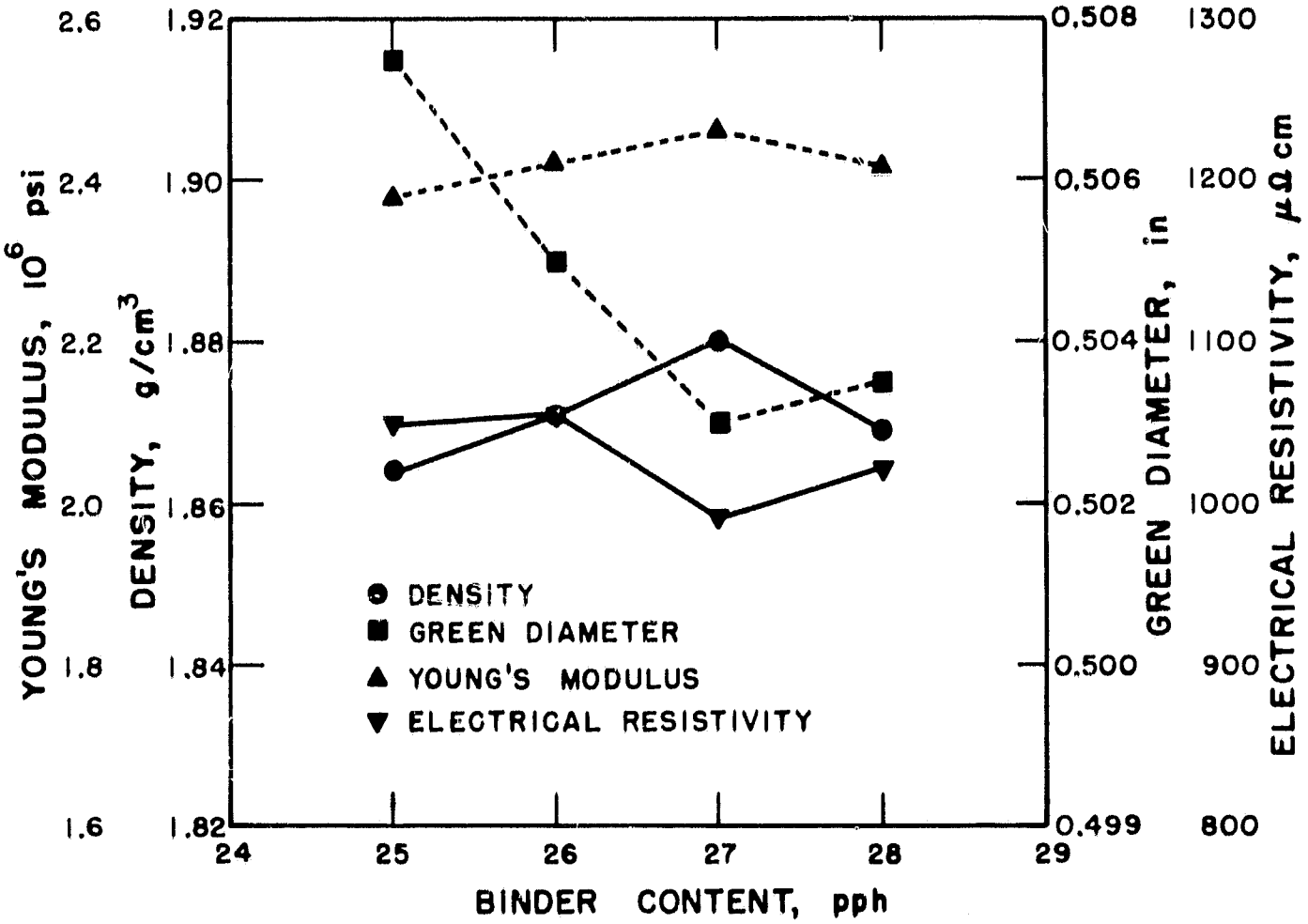

Fig. 16. Effects of binder concentration on properties of ABD graphites.

concentration. The differences in internal structure responsible for the property variations were too subtle to be identified by either optical or electron microscopy. All graphites appeared to be similar, well mixed, and with normal types and concentrations of defects.

Green diameter of rods made from the "standard" mix containing 27 pph binder was near the maximum which has previously been observed using this formulation. The maximum variation from it (about 0.004 inch at 25 pph binder) was approximately the same as the fluctuation in diameter observed over a period of months among several other lots all made with this same filler mix and binder concentration. Since variations in binder level among these previous lots is believed normally to have been less than 0.1 pph, it appears that this is not the primary cause of variations in green diameter. However, the association of green diameter with other properties of the finished graphite is apparent.

TABLE IX

PORE "SIZE" STATISTICS FOR ABD GRAPHITES

Specimen No.	Binder Content pph	Total Porosity %	Porosity Accessible to 2600 psi Hg %	Pore "Size" Statistics $\bar{x}_3$	s^2_{x3}	g_{x3}	$\bar{d}_3$	$s^2_{d_3}$	g_{d_3}
ABD3-4	25	17.35	5.36	-.586	.405	-.268	.686	.601	2.51
ABD2-4	26	17.04	4.83	-.589	.616	.286	1.02	15	620
ABD1-4	27	16.84	3.83	-.696	.584	.051	.772	3.98	94
ABD4-4	28	17.26	4.29	-.537	.738	.470	1.19	18.5	716

3. Multiple Extrusion (Series ABC and Previous Series)

Early in the CMF-13 graphite program the problem of blending raw materials was investigated, and it was concluded that a final procedure involving three successive stages of extrusion with intermediate chopping of the mix gave good results. Additional studies of this type have recently been made, again using Great Lakes Grade 1008 graphite flour, but in this case from a newer lot (CMB-6 Lot M-3, CMF-13 Lot G-18) which was somewhat more acicular than was that previously used (which was CMF-13 Lot G-13, taken from CMB-6 Lot M-2).

All specimens in the new, ABC series were made from a mix containing 85 parts G-18 graphite flour, 15 parts Lot TP-4 Thermax carbon black (which is believed to be identical with Lot TP-3 used previously), and 27 parts Varcum binder containing 4% maleic anhydride catalyst. The mix was extruded as 0.5-in. dia rods which were cured to 200°C in a 72-hr cycle (Cam No. 12), baked to 900°C in a 60-hr cycle (Cam No. 16), and graphitized to 2830°C in 6 hr. All graphites in the series were made by chopping the mix five times before the first extrusion and twice before each succeeding extrusion. The number of successive extrusions and properties in the cured, baked, and graphitized conditions are listed in Tables XII and XIII, which are to be compared with the results of earlier experiments summarized in Tables X and XI.

In previous experiments using G-13 graphite flour (Tables X and XI), good correlations were found between the amount of final mixing (chopping and extrusion) and both bulk density (Fig. 17) and Young's modulus (Fig. 18). Density and modulus rose quite rapidly with the first few extrusions, then more slowly with additional extrusions. The point in each figure plotted beyond the tenth extrusion, labelled "21-3", indicates the result of a mixing procedure involving 21 chops in advance of the first of

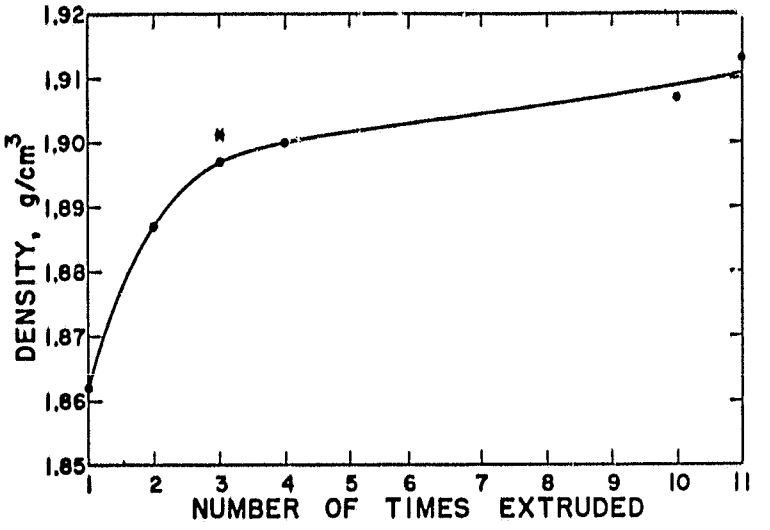

Fig. 17. Density of multiply extruded graphite rods made with G-13 flour.

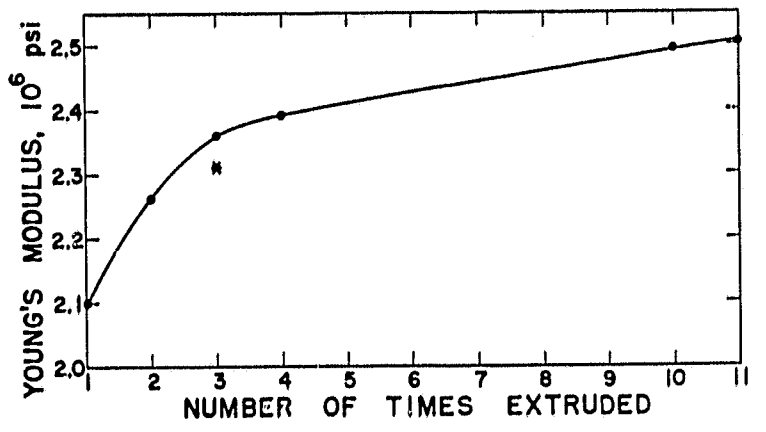

Fig. 18. With-grain Young's modulus of multiply extruded graphite rods made with G-13 flour.

TABLE X

PROPERTIES OF MULTIPLY EXTRUDED GRAPHITES (G-13 FLOUR)

Specimen Number	Mixing	Density g/cm^3	Young's Modulus 10^6 psi	Electrical Resistivity $\mu\Omega$ cm	Crystalline Anisotropy M	Crystalline Anisotropy σ_{ox}/σ_{oz}
AAD8-2	2 chops, 1 Ext.	1.862	2.10	1138		
AAD8-4	2 chops, Ext. 2 chops, Ext.	1.887	2.26	1073	1.33	1.61
AAD8-6	2 chops, Ext. 2 chops, Ext. 5 chops, Ext.	1.897	2.36	1070	1.36	1.65
AAD8-8	2 chops, Ext. 2 chops, Ext. 2 chops, Ext. 5 chops, Ext.	1.900	2.39	1063	1.36	1.61
AAB8-4	10 Ext. with 2 chops preceding each	1.907	2.49	1111	1.42	1.83
AAD6-6	21 chops, Ext. 2 chops, Ext. 2 chops, Ext. 2 chops, Ext.	1.913	2.5	1064	1.39	1.65
AAQ1	5 chops, Ext. 2 chops, Ext. 2 chops, Ext.	1.901	2.31	1160	1.36	1.64

TABLE XI

POROSITY OF MULTIPLY EXTRUDED GRAPHITES (G-13 FLOUR)

Specimen Number	Times Extruded	Total Porosity %	Porosity Accessible to 2600 psi Hg %	Pore "Size" Statistics $\bar{X}_3$	S^2_{x3}	g_{x3}	$\bar{d}_3$	S^2_{d3}	g_{d3}
AAD8-2	1	17.61	4.47	-0.22	0.69	-0.38	1.20	5.36	132
AAD8-4	2	16.50	3.04	-0.55	0.87	1.15	1.52	34.2	1369
AAD8-6	3	16.06	2.43	-0.82	0.83	1.66	1.33	33.6	1367
AAD8-8	4	15.93	2.71	-0.77	0.78	1.33	1.24	27.4	1080
AAB8-4	10	15.62	3.48	-0.85	0.77	2.12	1.37	31.4	1088
AAD6-6	21 chops, 3 Ext.	15.35	2.04	-0.95	0.97	2.62	1.57	46.7	1912

TABLE XII

PROPERTIES OF MULTIPLY EXTRUDED GRAPHITE (G-18 FLOUR - ABC SERIES)

Specimen Number [a]	Times Extruded	Density	Binder Carbon Residue	Young's Modulus 10^6 psi	Electrical Resistivity $\mu\Omega$ cm	Compressive Strength psi	Crystalline Anisotropy M [b]	Crystalline Anisotropy σ_{ox}/σ_{oz} [c]
ABC1-1-C	1	1.834	85.3±.1					
B		1.811±.001	47.5±.1					
G		1.854±.001	45.8±.1	2.343±.008	1118±14	8250±700	2.06	1.470
ABC1-2-C	2	1.855±.003	85.7±.2					
B		1.834±.005	48.7±.2					
G		1.877±.001	47.0±.2	2.468±.02	1021±23	7950±800	2.24	1.470
ABC1-3-C	3	1.860±.003	86.0±.3					
B		1.839±.005	49.8±.2					
G		1.882±.002	47.9±.2	2.488±.03	1020±112	7850±500	2.12	1.505
ABC1-4-C	4	1.858±.004	86.5±.1					
B		1.839±.006	50.1±.2					
G		1.882±.005	48.2±.2	2.546	966±33	8300±500	2.29	1.507
ABC1-5-C	5	1.857±.004	86.8±.2					
B		1.837±.002	50.3±.1					
G		1.891±.004	48.5±.1	2.585±.02	984±37	8250±400	2.35	1.512
ABC1-6-C	6	1.855±.001	87.4±.2					
B		1.835±.005	50.5±.4					
G		1.879±.004	48.6±.4	2.529±.02	1044±46	8500±300	2.07	1.518

(a) C, B, and G indicate cured, baked, and graphitized conditions respectively.

(b) M values approximately ±0.12.

(c) σ_{ox}/σ_{oz} values approximately ±0.01.

TABLE XIII

POROSITY OF MULTIPLY EXTRUDED GRAPHITES (G-18 FLOUR - ABC SERIES)

Specimen Number	Times Extruded	Total Porosity %	Porosity Accessible to 2600 psi Hg	Pore "Size" Statistics $\bar{x}_3$	s^2_{x3}	g_{x3}	$\bar{d}_3$	s^2_{d3}	g_{d3}
ABC1-1	1	18.0	5.7	-0.23	0.97	-0.11	1.41	8.73	202.
ABC1-2	2	17.0	3.8	-0.60	0.60	0.55	1.00	9.39	229.
ABC1-3	3	16.8	4.0	-0.60	0.81	0.55	1.05	8.48	204.
ABC1-4	4	16.7	4.3	-0.70	0.58	0.41	0.88	7.68	192.
ABC1-5	5	16.4	4.5	-0.84	0.85	-0.77	0.72	4.20	101.
ABC1-6	6	16.7	4.9	-0.64	0.75	1.19	1.30	28.	1100.

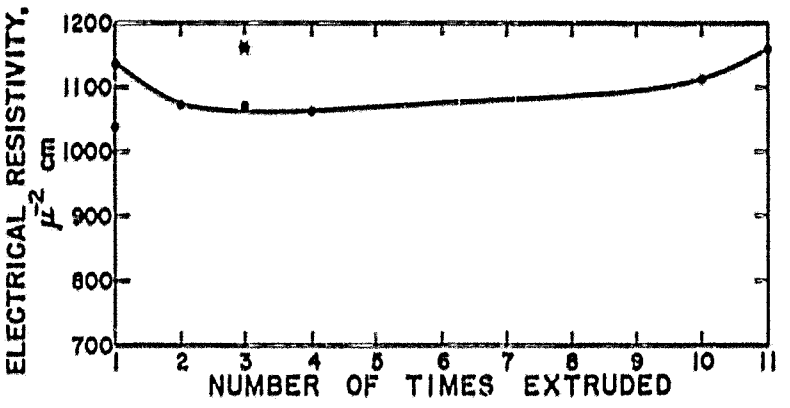

Fig. 19. With-grain electrical resistivity of multiply extruded graphite rods made with G-13 flour.

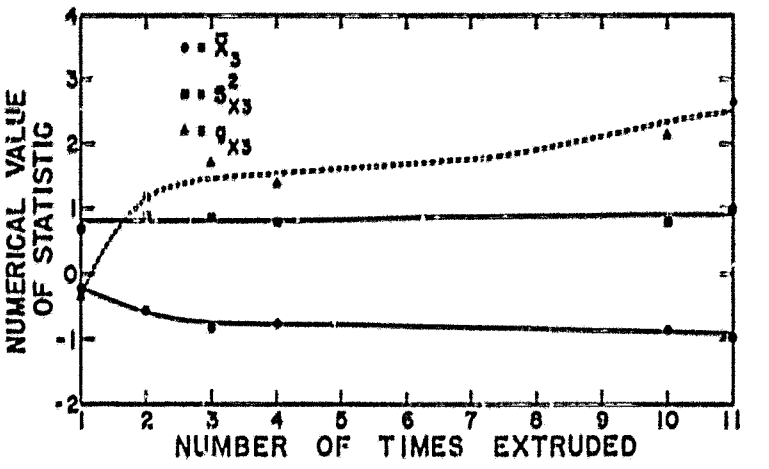

Fig. 21. Logarithmic pore "size" statistics for multiply extruded graphite rods made with G-13 flour.

three extrusions, and is located arbitrarily with regard to the abscissa. The asterisks indicate data for AAQ1 graphite, which was mixed by a procedure similar to that represented on the abscissa by "3 times extruded" but which involved three additional chops in advance of the first extrusion.

Electrical resistivity changed only slightly with repeated extrusion (Fig. 19), but appeared to decrease slightly as a result of the second extrusion and to increase slightly between the fourth and tenth extrusions.

Porosity was measured by mercury porosimetry and pore "size" distribution statistics were calculated using the FININT code. Both calculated total porosity and porosity accessible to mercury at 2600 psi are plotted in Fig. 20. Accessible porosity is a minimum at three extrusions, but total porosity continues to decrease slowly with additional extrusions. The point representing 21 chops and 3 extrusions was the lowest with regard to both total and accessible porosities, suggesting that after the first few extrusions the chopping operation is more effective in reducing porosity than is repeated extrusion. Pore "size" statistics are plotted in a logarithmic form (as they are calculated initially) in Fig. 21, and on the basis of a linear "pore diameter" in microns, derived from the logarithmic values, in Fig. 22. $\bar{X}_3$ decreases slowly with each successive extrusion while S^2_{X3} increases slightly, indicating a decreasing average pore "size" and a broadening distribution of pore "sizes". In terms of $\bar{d}_3$, however, it appears that average pore "size" is increasing slightly while the breadth of the distribution increases drastically. The trends indicated by the logarithmic data of Fig. 21 are probably the more reliable, since these curves are based more directly on experimental measurements.

Crystalline anisotropy is plotted as a function of number of extrusions in Fig. 23. Anisotropy is represented

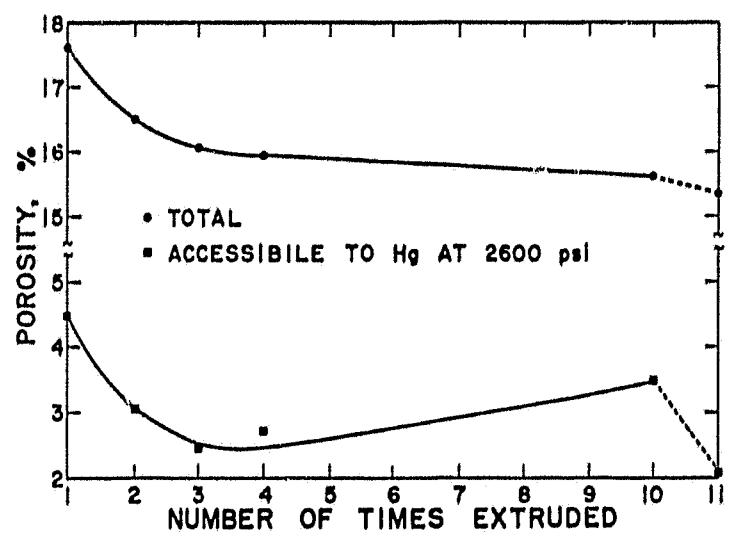

Fig. 20. Total and accessible porosity of multiply extruded graphite rods made with G-13 flour.

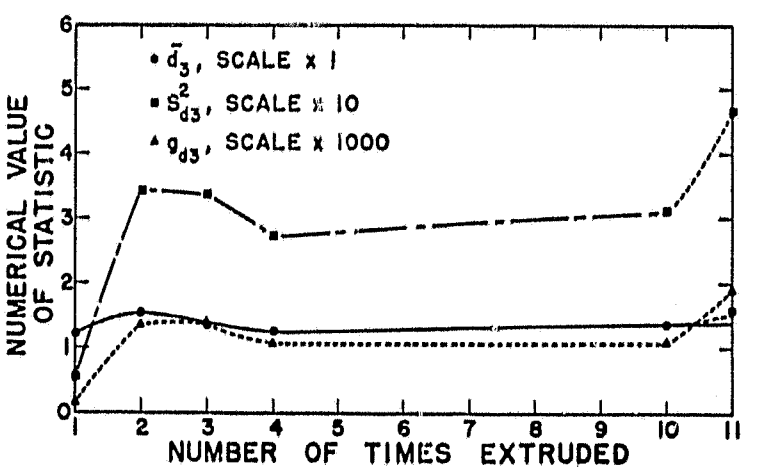

Fig. 22. Linear pore "size" statistics for multiply extruded graphite rods made with G-13 flour.

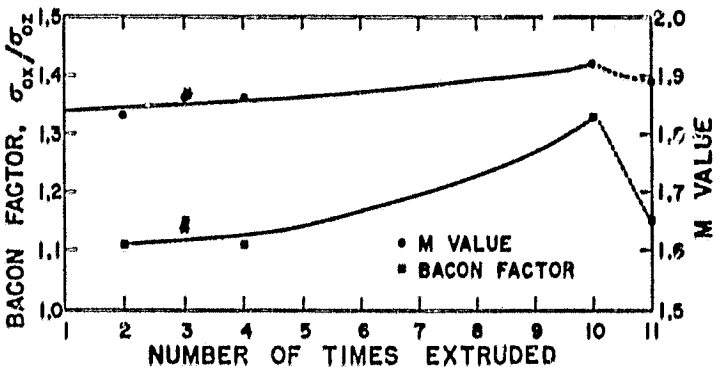

Fig. 23. Crystalline anisotropies of multiply extruded graphite rods made with G-13 flour.

both by an M value, where M is the exponent of the cosine in the cosine function which best represents the intensity distribution in the diffracted x-ray beam, and by the Bacon anisotropy factor, σ_{ox}/σ_{oz}. Both indicate a gradual increase in degree of preferred orientation with repeated extrusion. The points representing material prepared using 21 chops and 3 extrusions would fit the curves much better at 3 extrusions than they do as they have actually been plotted, suggesting that degree of preferred orientation is influenced more by the extrusion operation than by chopping.

When a resin binder of the Varcum type is used, the mix "dries out" during repeated extrusion and finally becomes too dry to extrude properly. This usually occurs somewhere between the fifth and the tenth extrusion, depending on such factors as temperature of the mix during chopping and extrusion, the proportion of binder used, the amount of solvent added to the binder, if any, and the humidity of the room. There is no straightforward way to evaluate thi. variable or its effects.

The new ABC series of multiply extruded graphite rods was made using the more acicular G-18 graphite flour and with acetone to dilute the binder. The mix was overly dry for the sixth extrusion, which is probably responsible for changes in the trends of several of the curves shown below.

Densities of the ABC graphites in the cured, baked, and graphitized conditions are plotted in Fig. 24. In all conditions density increased sharply with the first few extrusion passes, levelled off, then finally decreased a little. Binder carbon residue, plotted in Fig. 25, in-

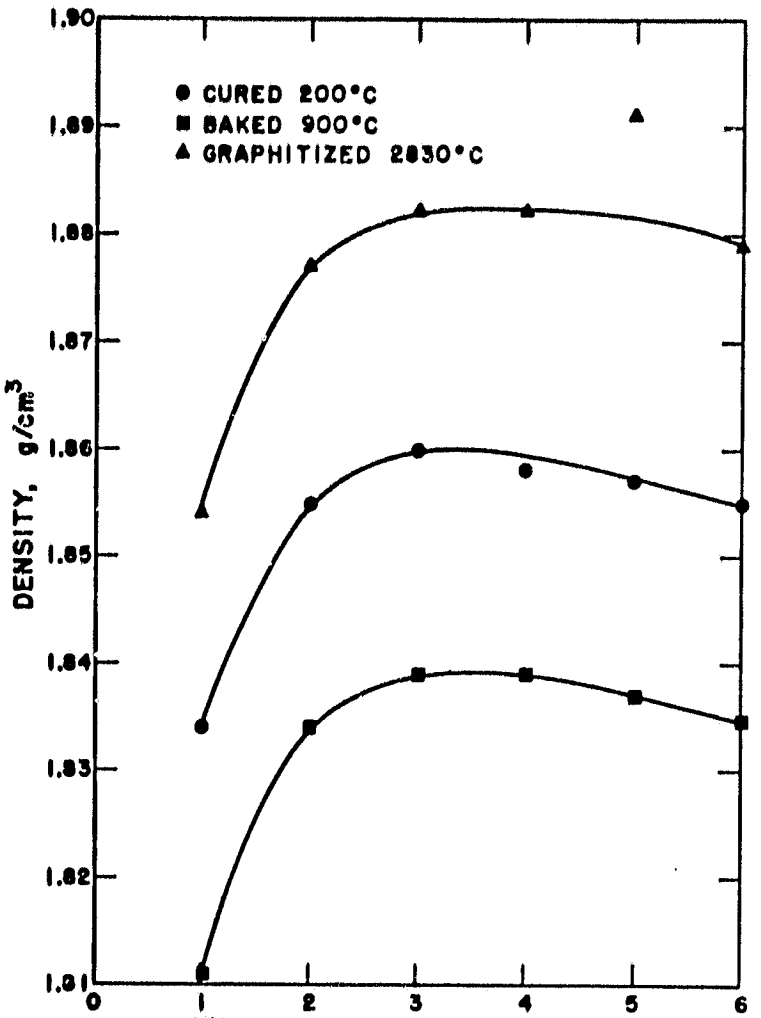

Fig. 24. Densities of multiply extruded graphite rods made with G-18 flour.

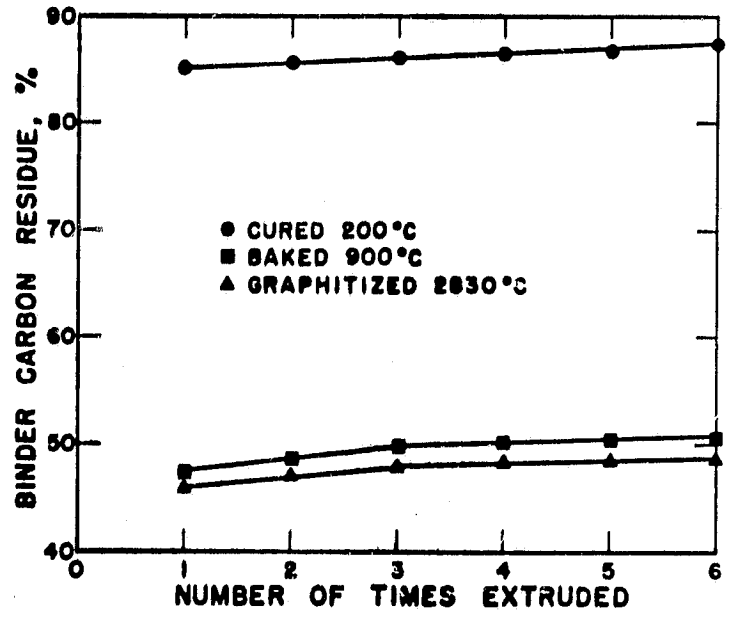

Fig. 25. Binder carbon residues in multiply extruded graphite rods made with G-18 flour.

creased linearly with number of extrusions for the cured state and at a diminishing rate for the baked and graphitized conditions. The increase in carbon residue is not enough in any case to account for the corresponding increase in density, so that much of the density increase must be attributed to improved packing of filler particles as a result of multiple extrusion.

Electrical resistivity, plotted in Fig. 26, had a minimum value at about the fourth extrusion pass. Both the average value and the standard deviation shown for rods extruded three times are probably high due to one rod which had abnormally high resistivity.

Degree of preferred orientation (Fig. 27) was distinctly higher than for graphites made from G-13 flour, and increased smoothly with number of extrusion passes to the sixth pass, which was probably disturbed by excessive dryness of the mix. Both with-grain electrical resistivity (Fig. 26) and with-grain Young's modulus (Fig. 28) reflect the changes in preferred orientation. With-grain resistivity was distinctly lower and with-grain modulus appreciably higher than for equivalent graphites made from G-13 flour.

Compressive strength (Fig. 29) was measured using only three specimens to represent each extrusion condition, and data scatter was broad. Standard deviations overlap for all conditions, and it is not clear that there was any real change in compressive strength with repeated extrusion.

Total and accessible porosities for the ABC series are plotted in Fig. 30. They show the same trends evident in Fig. 20 for graphites made with G-13 flour, but

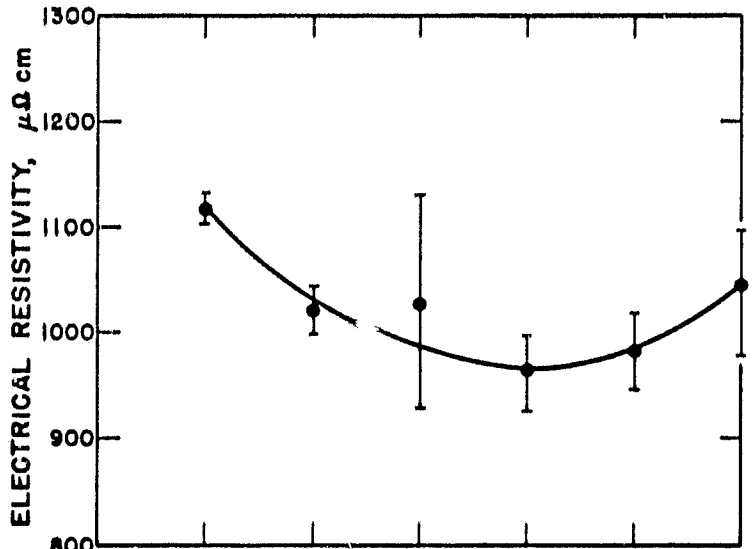

Fig. 26. With-grain electrical resistivity of multiply extruded graphite rods made with G-18 flour.

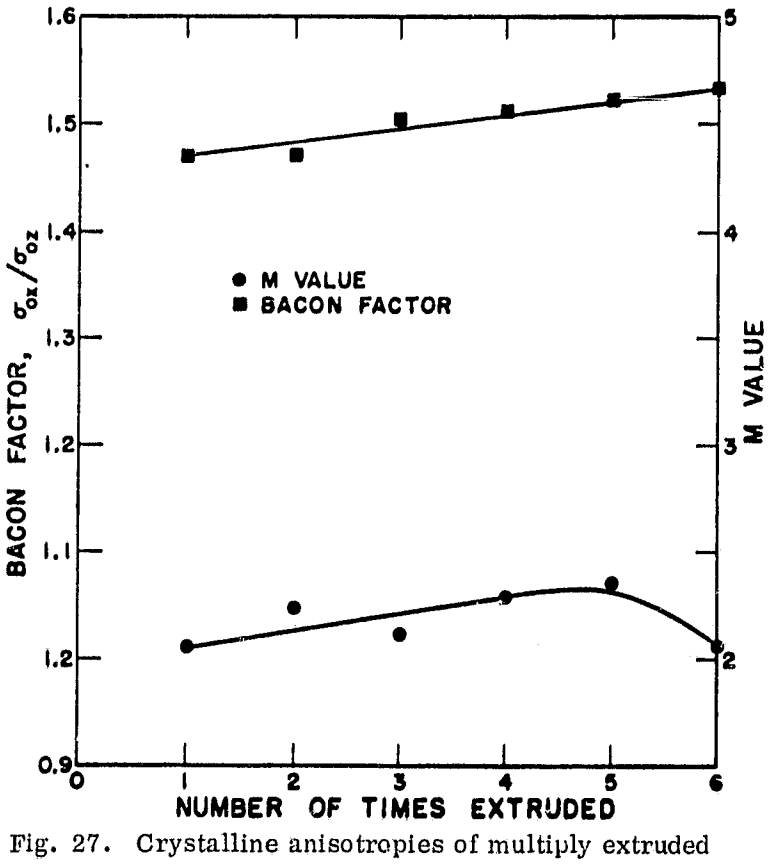

Fig. 27. Crystalline anisotropies of multiply extruded graphite rods made with G-18 flour.

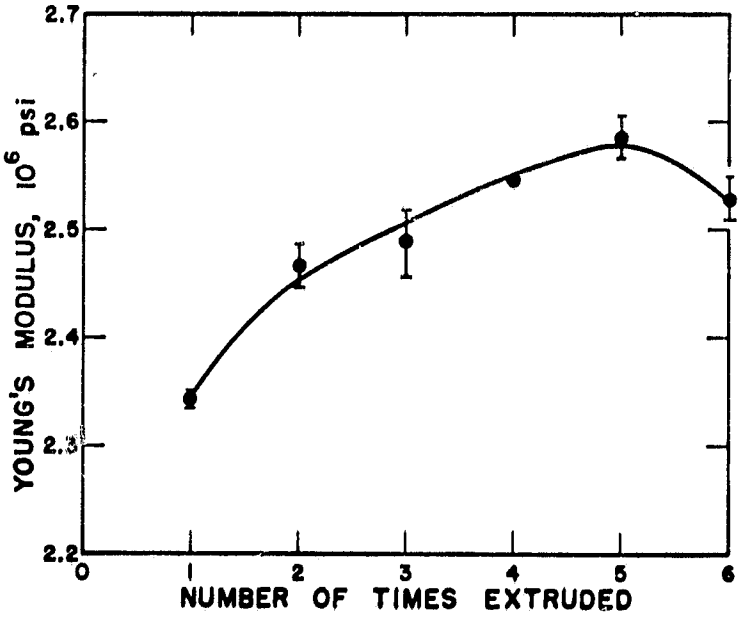

Fig. 28. With-grain Young's modulus of multiply extruded graphite rods made with G-18 flour.

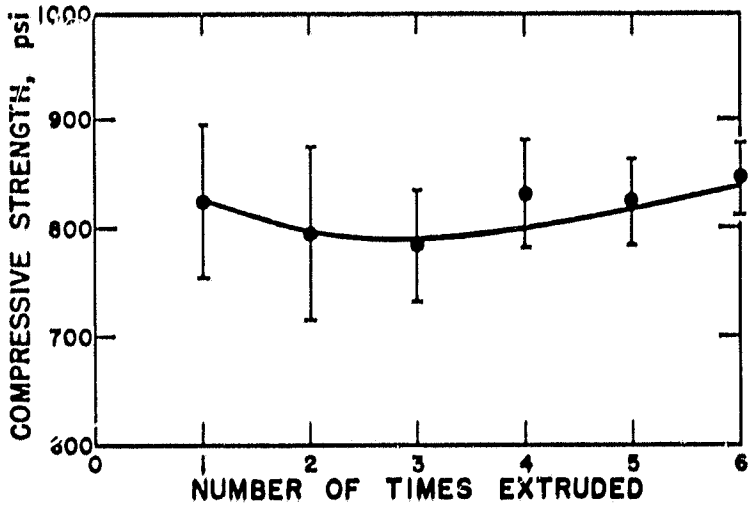

Fig. 29. With-grain ultimate compressive strength of multiply extruded graphite rods made with G-18 flour.

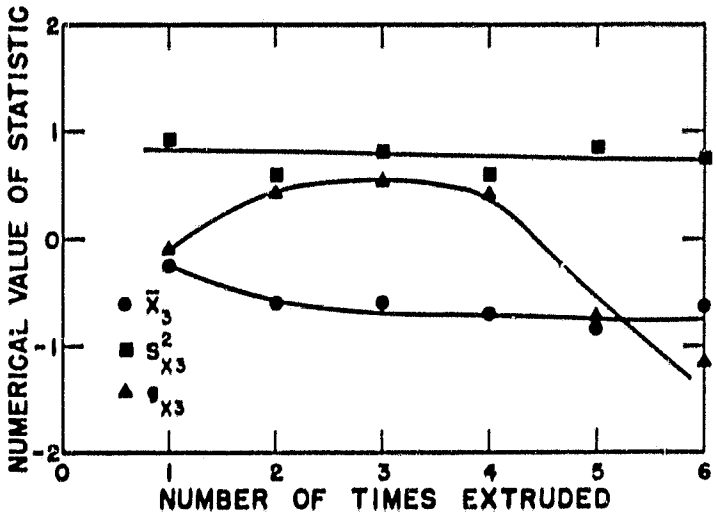

Fig. 31. Logarithmic pore "size" statistics for multiply extruded graphite rods made with G-18 flour.

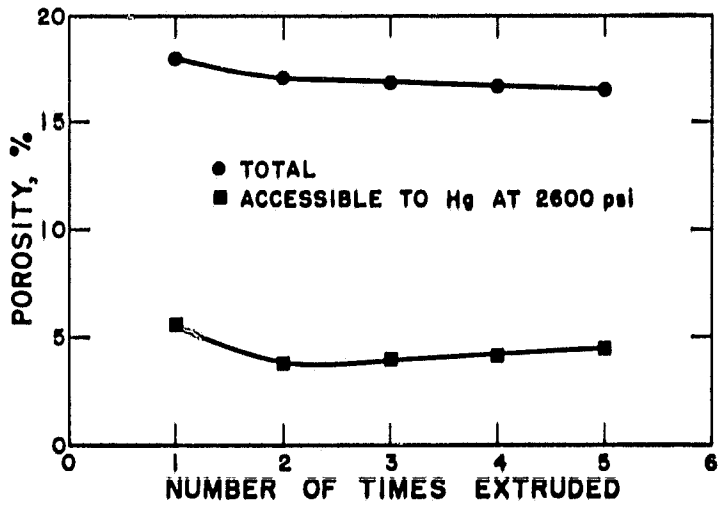

Fig. 30. Total and accessible porosity of multiply extruded graphite rods made with G-18 flour.

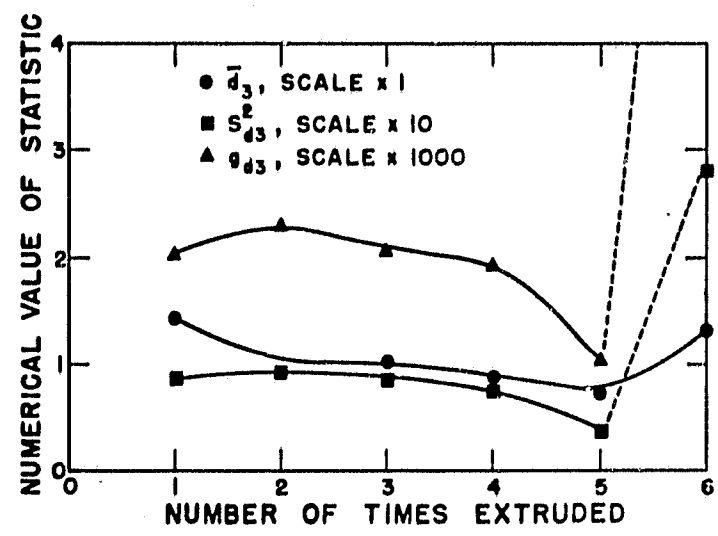

Fig. 32. Linear pore "size" statistics for multiply extruded graphites made with G-18 flour.

are higher in both total and accessible porosity. Pore "size" statistics for the ABC graphites are summarized in Fig. 31 and 32. As indicated by $\bar{X}_3$, pore "size" decreases with repeated extrusion, with little change in the breadth of the distribution (represented by the variance, S^2_{x3}). In this case, the linear parameters (Fig. 32) showed generally similar trends, but with unreasonable values after six extrusions -- probably again originating in excessive dryness of the mix, but exaggerated by the data treatment.

Microstructural differences among graphites of the ABC series were too subtle to be detected by either optical or electron microscopy. All appeared well mixed and were partially penetrated by the epoxy mounting resin, indicating some degree of interconnection of porosity. Some c-face cracks, void colonies, and stringers of voids along large filler particles were observed, but in only normal sizes and concentrations.

Summarizing the data from both series of multiple extrusions, it can be concluded that, at least for this type of graphite and this section size:

(a) The principal useful properties of the graphite are improved by repeated extrusion up to the point at which the mix becomes excessively dry, which with normal handling occurs after about five extrusions.

(b) This improvement is represented by increases in density, Young's modulus and binder carbon residue, and decreases in electrical resistivity and accessible porosity. These changes are accompanied

by an increase in degree of preferred orientation, and so by increasing anisotropy of structure and properties.

(c) For most purposes the optimum number of times to extrude appears to be three, although for special purposes either two or four extrusions may be preferred.

(d) Chopping the mix a large number of times has the same effect in increasing density and decreasing accessible porosity as has repeating the extrusion operation, but does not increase the degree of preferred orientation.

D. Copolymer Binders (J. M. Dickinson)

Experimental extruded graphites of the ABF series were made to investigate the behavior as binders of a group of furfuryl alcohol-formaldehyde copolymer resins. These resins were synthesized by E. M. Wewerka, CMF-13, and covered a wide range of compositions and viscosities.

The filler used was a mixture of 85 parts G-18 graphite flour and 15 parts TP-4 Thermax carbon black and binder concentration was held constant at 27 pph. Binder descriptions and extrusion conditions are summarized in Table XIV. (The "FA/HCOH ratio" indicates the relative proportions in which furfuryl alcohol and formaldehyde were mixed in preparing the resin.) Extrusion pressure appears to be directly related to binder viscosity, and green diameter inversely related to binder viscosity. No relation was evident between FA/HCOH ratio and extrusion parameters.

Extruded rods were cured at 2.5°C/hr to 420°C, baked to 900°C in 60 hr, and graphitized to 2830°C in 6 hr. Carbon residues in the cured, baked and graphitized conditions are listed in Table XV, together with properties of the graphitized rods. Carbon residues were somewhat lower than would be expected in similar graphites made with a normal furfuryl alcohol resin such as Varcum. Densities were also somewhat lower, with the possible exception of Lot ABF10. Graphites made from resins having 1/1 and 2/1 ratios of furfuryl alcohol to formaldehyde had lower densities than did comparable graphites made from resins having a 20/1 ratio. It appears that still higher ratios should be investigated.

Microstructural examinations of extruded rods in the cured condition showed a dense, well-mixed material, perhaps slightly deficient in fine filler particles. After graphitizing, microstructures were much like those observed in similar graphites made from furfuryl alcohol resins, but with more visible porosity. Specimen ABF4 contained a number of central cracks, probably caused by an excessively high rate of gas evolution during curing or baking. Specimens ABF10 and ABF11 showed zones of interparticle cracking extending inward about 250 to 500μ from cylindrical surfaces.

Because of the presence of carbon-black particles in the binder residues, no evidence on the tendency of these binders to graphitize could be collected by optical or elec-

TABLE XIV

BINDER DESCRIPTIONS AND EXTRUSION CONDITIONS, ABF GRAPHITES

Specimen Number	Binder Description: Identification	Binder Description: FA/HCOH ratio	Binder Description: Viscosity cp	Extrusion Conditions: Pressure psi	Extrusion Conditions: Speed in./min	Extrusion Conditions: Temp. °C	Extrusion Conditions: Green Dia., in.
ABF 4	EW197	1/1	1200	9300	171	47	0.5005
ABF 8	EW205	2/1	366	5400	171	43	0.506
ABF 9	EW206	20/1	355	5400	176	40	0.506
ABF 10	EW207	20/1	645	8300	171	48	0.5025
ABF 11	EW212	2/1	1623	9500	164	51	0.501

TABLE XV

PROPERTIES OF ABF GRAPHITES

Specimen Number	Condition	Carbon Residue %	Young's Modulus 10^6 psi	Electrical Resistivity $\mu\Omega$ cm	Density g/cm^3	Compressive Strength psi
ABF 4	Cured	60.2±1.1				
	Baked	45.9±1.1				
	Graphitized	43.9±1.1	2.640±.02	990±27	1.838±.003	9576±420
ABF 8	Cured	61.9±.1				
	Baked	47.1±.1				
	Graphitized	45.4±.1	2.53±.03	1184±5	1.844±.003	---
ABF 9	Cured	64.1±.2				
	Baked	49.0±.1				
	Graphitized	47.0±.4	2.31±.02	1212±6	1.855±.003	---
ABF 10	Cured	63.7±1.9				
	Baked	48.8±1.7				
	Graphitized	47.0±1.7	2.57±.07	1126±19	1.894±.008	---
ABF 11	Cured	62.7±1.6				
	Baked	47.6±1.5				
	Graphitized	46.7±1.5	2.65±.08	1150±23	1.855±.012	---

tron microscopy. A series of molded specimens was therefore made in which these copolymers were used as binders at concentrations of 27 and 58 pph and the filler was G-18 flour only, with no Thermax addition. These were made at low pressure, and were in general very porous. After graphitization, the binder residues were in general indistinguishable from the filler particles by either optical or electron microscopy. They had well-developed lamellar structures and strong optical anisotropy, indicating that in the presence of the G-18 filler particles all of these binders had graphitized very well.

VII. STRUCTURAL STUDIES

A. Carbon Blacks

1. Electron Microscopy (L. S. Levinson)

Six lots of carbon black, listed in Table XVI, have been purchased from Cabot Carbon Co. An attempt was made to disperse a sample of each ultrasonically for examination by direct-transmission electron microscopy. In agreement with the observations of Dr. F. A. Heckman, head of the Cabot Co.'s microscopy section, it was found to be impossible to disperse any of them into discrete particles, and so particle counting was not attempted. However, the observed particle diameters were consistent with the nominal particle sizes reported by the Cabot Co., which are listed in Table XVI.

2. X-ray Diffraction (J. A. O'Rourke)

Crystalline parameters of the six Cabot carbon blacks, as-received and after heat-treating for 30 min at 2820°C, are listed in Table XVI. All showed some degree of graphitization as a result of heat treatment, and the two Sterling Grades (Samples T-7 and T-8) graphitized significantly. Carbolac 1 and Super Carbovar (Samples T-3 and T-4)

TABLE XVI

CRYSTALLINE PARAMETERS OF CABOT CARBON BLACKS

CMF-13 Lot No.	Grade	Condition	Particle[a] Size Å	L_c, Å	d_{002}, Å	Amorphous Carbon %	Unassociated Layers %	Component
T-3	Carbolac 1	As-received	50	11.9	3.45	29	13	---
---	Carbolac 1	0.5 hr @ 2820°C	--	15.4	~3.44	--	10	"Amorphous"
				~145	~3.42	--	--	Crystalline
---	Carbolac 1	1 hr @ 2820°C[b]	--	17.1	3.44	--	--	"Amorphous"
				105	3.40	--	--	Crystalline
T-4	Super Carbovar	As-received	140	9.5	3.53	35	9	---
---	Super Carbovar	0.5 hr @ 2820°C	---	23	~3.44	--	10	"Amorphous"
				~250	~3.41	--	--	Crystalline
---	Super Carbovar	1 hr @ 2820°C[b]	---	22.2	3.44	--	--	"Amorphous"
				100	3.40	--	--	Crystalline
T-5	Monarch 81	As-received	220	11.6	3.45	38	5.5	---
---	Monarch 81	0.5 hr @ 2820°C	---	44	3.44	--	--	---
T-6	Elftex 5	As-received	290	12.7	3.48	31	4.0	---
---	Elftex 5	0.5 hr @ 2820°C	---	58	3.44	--	--	---
T-7	Sterling 99	As-received	420	15.1	3.48	23	4.0	---
---	Sterling 99	0.5 hr @ 2820°C	---	100	3.405	--	--	---
T-8	Sterling FT	As-received	1690[c]	16.2	3.47	19	2.6	---
---	Sterling FT	0.5 hr @ 2820°C	---	210	3.387	--	--	---

(a) Nominal average particle diameter reported by Cabot Carbon Co.

(b) Two treatments of 30 min each at 2820°C.

(c) Measured mean particle diameter, from LA-3989-MS, page 5.

were quite fluffy and packed to very low densities in the sample holders, so that parameters reported for them are approximate only. After heat treatment both contained minor proportions of a more highly crystalline component, which was resolved graphically and is listed separately in the table. Both also still contained measurable fractions of single, unassociated carbon layers. They were therefore given a second 30-min heat-treatment at the same temperature, with the results shown in the table. A crystalline component was still apparent in both samples, but the diffraction peak representing it was broader and more intense than after the first heat treatment. A small proportion of unassociated single layers was still present in Sample T-4, but none were detected in Sample T-3.

B. Hot-Worked Pyrolytic Graphites (L. S. Levinson)

Two samples of pyrolytic graphite which had been swivelled at high temperatures in CMF-13 experiments have been examined to determine the orientation at which the microscopic appearance of a section changes from lamellar to scaly. Specimen T-34, for which preliminary results were reported in LA-3989-MS, showed this transition when the angle between the section and the average

layer-plane orientation was 45° to 46°. Specimen T-35, examined recently, showed the transition when the angle was 49° to 50°. Since these specimens were somewhat curved and were difficult to mount precisely, it is felt that these results represent reasonable agreement.

To determine the transition angle as accurately as possible, a larger, more nearly flat specimen of hot-pressed pyrolytic graphite has been obtained from Dr. J. T. Meers of Union Carbide Corporation's Parma Technical Center. This is a type of material now being marketed as monochromators for neutron and x-ray diffraction studies. The piece received by CMF-13 was stated to be slightly substandard for that application, but indeed was nearly perfect. X-ray measurements by J. A. O'Rourke, CMF-13, showed an essentially infinite crystallite size, a d-spacing of 3.356 Å (which corresponds to about 10 to 15% of disoriented layers), and an M-value over 300, indicating very little wrinkling of basal planes. Specimens prepared for transmission electron microscopy (using the Scotch-tape technique) were somewhat turbostratic, as indicated by moiré fringes and selected-area diffraction patterns. The moiré patterns showed evidence that dislocations were present. On a section cut at 45° to the average basal plane the structure was uniformly lamellar, with no indication of growth cones.

C. Fracture Path in ATL Graphite (L. S. Levinson)

Grade ATL is a pitch-bonded graphite of medium grain size and moderate density manufactured in very large sizes by Carbon Products Division of Union Carbide Corporation. A sample of ATL graphite broken in three-point bending was reassembled, mounted in a low-viscosity epoxy resin, and examined to determine the path followed by the fracture. In this graphite there are many relatively large voids both within and between filler particles, and the fracture path seemed largely to be from void to void. Because it contains particles of carbon black, the binder residue in ATL graphite is easily identified, and it was clear that the fracture path was in some places through binder residue, in some through filler particles, and in some along the interface between binder and filler. On the basis of a very limited sample, it appeared that the preferred fracture path was through filler particles where their lamellar and void structures produced a weak zone at a high angle to the tensile axis, and at the interface between filler and binder when weak zones within the particles were nearly parallel to the axis of tension.

VIII. PHYSICAL AND MECHANICAL PROPERTIES

A. Deformation Mechanisms (J. Weertman, E. G. Zukas, W. V. Green)

An analysis has been made of the stress and displacement-velocity fields around a crack in a material undergoing high-temperature creep. Both isotropic and anisotropic materials were considered, and the increase in creep rate caused by the presence of a high density of cracks was calculated. It was concluded that high crack density (which is normal in a graphite) increases creep rate in tension very much more than it does the creep rate in shear.

The growth kinetics of simulated cracks machined into the gage sections of ZTA graphite specimens have been studied in tensile creep tests. Displacement-time and displacement-position diagrams have been constructed, and will be compared with predicted displacement diagrams based on the analysis described above.

B. Activation Energy for Creep (W. V. Green, E. G. Zukas)

In recent experiments an attempt has been made to extend the determination of an activation energy for tensile creep to the lower limit of the temperature region in which creep occurs rapidly enough so that it can be observed accurately in a short-time test. Initial experiments were with Graph-i-Tite G at 2100°C. These were abandoned when it was discovered that the particular billet from which samples were taken had not been reimpregnated by the manufacturer, and so was not typical of this commercial grade. A second set of experiments was therefore undertaken in which the material tested was an experimental graphite, CMF-13 Lot AAQ1. By use of the change-in-temperature technique between 2100 and 2300°C, an activation energy for creep was determined which was

approximately the same as that previously determined at higher temperatures. However, strain to tensile fracture of this graphite is small (less than 1%) in this temperature range, and uncertainties in strain measurements -- on which the calculation of activation energy is based -- were therefore relatively large. The determination will be repeated in a third series of tests on ATJ graphite which, it is hoped, will sustain at least 1 to 2% of tensile creep strain at each of the temperatures of interest.

C. Thermal Conductivity (P. Wagner)

1. Boronated Graphites

For metals, and for degenerate systems in general, the electronic component of thermal conductivity, k_e, is related to electrical conductivity, σ, by the equation:

$$k_e = \frac{\pi^2}{3} \left(\frac{k_B}{e}\right)^2 \sigma T = 2.45 \times 10^{-8} \sigma T ,$$

where k_B is the Boltzmann constant and e is the charge on the electron. The ratio k_e/σ at a particular temperature is, therefore, a constant for all such systems.

To a good approximation, the total thermal conductivity, k, of a graphite can be expressed as the sum of a lattice component and an electronic component:

$$k = k_L + k_e .$$

For graphite at a particular temperature, the ratio $k/\sigma = (k_L + k_e)/\sigma$ is several hundred times as great as for a metal at the same temperature. Since k_e/σ is assumed to be the same in the two types of materials, this suggests that k_L/σ is very large in graphite, and that in graphite most of the thermal energy is transported by the lattice. However, the relationship between k_L and k_e in graphite has not yet been reported in the literature.

Interest in this relationship is two-fold. First, there has been considerable speculation that electronic transport processes in graphite are enhanced by a bipolar diffusion mechanism, but proof of this must await a measurement of k_e. Second, knowledge of k_L is required to compute in-plane crystallite dimensions (L_a) from thermal-conductivity measurements. A means of separating k, which is routinely measured, into its two components is therefore being sought.

It has been reported (Hove, J. E., Conf. on Industrial Carbon and Graphite, London, Sept. 1957) that the addition of boron to graphite changes its electrical conductivity -- and thus k_e -- without affecting k. If this were correct, it should be possible to deduce the relationship of k_L to k_e by comparisons of the electrical and thermal properties of a series of graphites containing controlled amounts of boron. Accordingly, the series of extruded, resin-bonded graphites listed in Table XVII was made, using the same raw materials and manufacturing conditions throughout except for small additions of finely-divided metallic boron to the raw mixes. Results of with-grain measurements of electrical resistivity and thermal conductivity are listed in the same table and plotted in Fig. 33. Standard deviations of the electrical-resistivity measurements, which are very sensitive to structure, are also listed in the table, to demonstrate the remarkable uniformities of the boronated graphites.

As was expected, electrical conductivity of the graphite, σ, increased with increasing boron content. Unexpectedly, however, thermal conductivity, k, diminished.

TABLE XVII

WITH-GRAIN ELECTRICAL RESISTIVITIES AND THERMAL CONDUCTIVITIES OF BORONATED GRAPHITES AT 300°K

Lot No.	Boron Content, %	ρ, μΩ cm	k, w/cm-°K
AAM-12	0.000	1068, σ= 3.1%	1.14
AAM-5	0.000	1076 ---	---
AAM-10	0.022	1071, σ= 3.2%	1.11
AAM-9	0.039	957, σ= 1.6%	1.10
AAM-6	0.041	1064, σ= 0.5%	1.07
AAM-11	0.062	875, σ= 3.9%	0.99
AAM-7	0.081	875, σ= 0.4%	0.98
AAM-8	0.158	766, σ= 0.6%	0.80

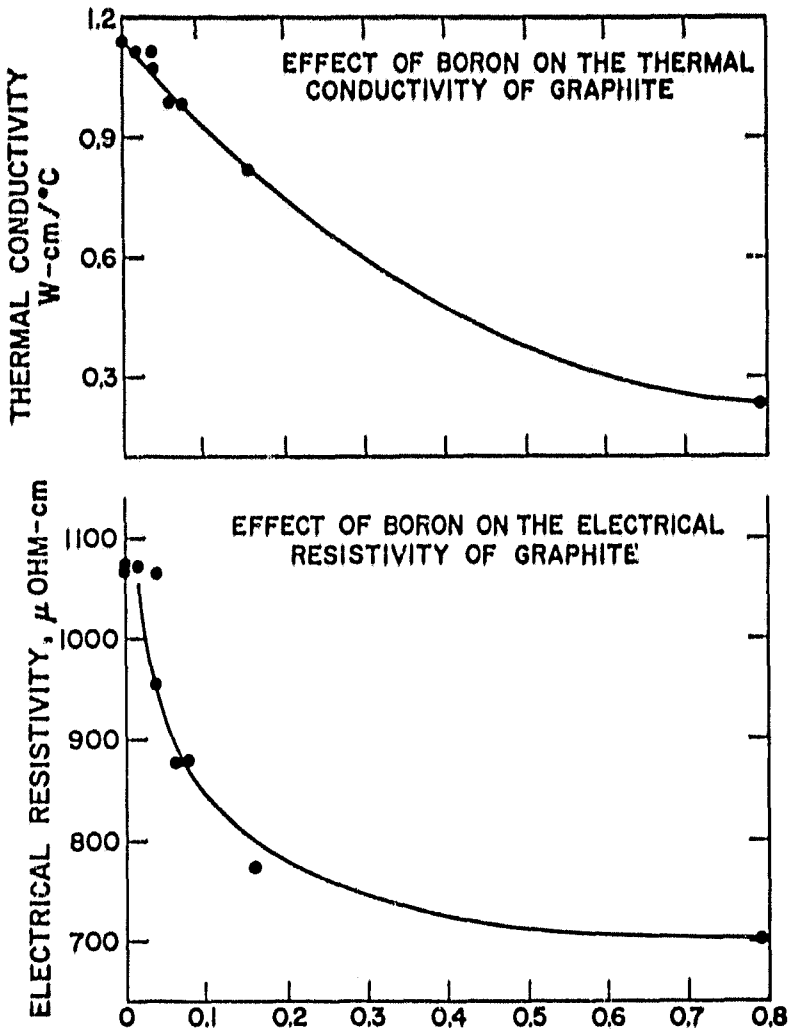

Fig. 33. Thermal conductivities and electrical resistivities of boronated graphites.

X-ray diffraction measurements by J. A. O'Rourke, CMF-13, showed that d_{002}, the layer spacing of the graphite, did not change with boron additions over the composition range considered, and produced no evidence for the presence of boron carbide. Apparently boron atoms have substituted for carbon atoms in the layer planes of the graphite structure, increasing the number of electrical charge carriers but degrading the periodicity of the lattice and reducing the lattice component of thermal conductivity.

It is possible that very small boron additions ($<<0.1\%$) may produce a system in which electrical properties vary while phonon transport is unaffected. It is apparent, however, that in such a system the changes in electrical resistivity would be too small to measure with the accuracy required to deduce the relationship of k_L to k_e. Boronated graphites, therefore, will not be further studied at this time for that purpose. The possibility of using small boron additions to reduce electrical resistance and increase uniformity of properties remains interesting for other purposes.

2. Silicon-Doped Graphites

A group of extruded, resin-bonded graphites, listed in Table XVIII, was made in which silicon was added in small amounts in the hope that, unlike boron, it might affect electrical conductivity without altering thermal conductivity. As can be seen from the average properties listed in the table, over the range of concentrations considered silicon had no systematic effect on these properties.

3. Pyrolytic Carbon

An attempt was made to determine the thermal conductivity of a pyrocarbon specimen manufactured by LASL Group CMB-8 and of interest to LASL Group K-4. Since the specimen was only 0.028 cm thick, the best that could be done was an estimate based on flash-diffusivity measurements, which gave a value of $k = 0.08$ w/cm-°C. This material was less anisotropic than was a specimen previously tested, for which $k = 0.014$ w/cm-°C. The relative values appear to be reasonable.

D. Properties of POCO Graphites (P. Wagner)

Density, electrical resistivity, and thermal conduc-

TABLE XVIII

WITH-GRAIN ELECTRICAL RESISTIVITIES AND THERMAL CONDUCTIVITIES OF SILICON-DOPED GRAPHITES AT 300°K

Lot No.	Silicon Content, %	ρ, μΩcm	k, w/cm-°C
AAM-16	0.000	1131	1.33
ABH-1	0.045	1141	1.24
ABH-2	0.20	1146	1.26
ABH-3	0.59	1122	1.28

TABLE XIX

ROOM-TEMPERATURE PROPERTIES OF POCO GRAPHITES

Grade Designation	Condition	Density, g/cm³	Electrical Resistivity μΩ-cm		Thermal Conductivity w/cm-°C	
			WG	AG	WG	AG
AXZ	Graphitized to 2300°C	1.55	2163	2159	.58	.57
AXZ-QB	Impregnated, not regraphitized	1.62	1984	2030	.56	.55
AXZ-QBG	Impregnated, regraphitized	1.61	1891	1994	.67	.65
AXZ-9Q	Graphitized to 2900°C	1.55	2202	2114	.61	.55
AXF	Graphitized to 2300°C	1.84	1586	1571	.82	.83
AXF-QB	Impregnated, not regraphitized	1.88	1551	1558	.90	.89
AXF-QBG	Impregnated, regraphitized	1.87	1418	1460	.95	.94
AXF-9Q	Graphitized to 2900°C	1.81	1375	1429	.99	.96

tivity have been measured at room temperature on specimens taken from billets of eight commercial graphites manufactured by POCO Graphite, Inc., with the results listed in Table XIX. The two basic grades represented are AXZ, their lowest density standard grade, and AXF, their highest density standard grade. Both are normally graphitized only to 2300°C. The effects of graphitizing to 2900°C, of impregnating without regraphitizing, and of impregnating and regraphitizing are supposedly illustrated for both grades by the samples listed. If these samples are typical, graphitizing to 2900°C instead of 2300°C had essentially no effect on Grade AXZ, but significantly reduced density and resistivity of Grade AXF, and increased its thermal conductivity. For both basic grades, impregnation (without subsequent graphitization) increased density and thermal conductivity and reduced electrical resistivity. Graphitization of the impregnated material then reduced density slightly, reduced electrical resistivity further, and further increased thermal conductivity. The measured densities of the samples of AXZ, AXF and AXF-QB were within the ranges listed by the manufacturer's advertising literature, while that of the AXZ-QB was below the listed range. Electrical resistivities of all four of these grades were below the ranges listed by the manufacturer.

The structures and properties of these graphites are being explored further.

E. Thermal Shock (D. T. Eash, P. E. Armstrong)

As has been indicated above, calculated thermal shock indices are generally agreed to have only qualitative usefulness in indicating resistance of a given material to thermal shock (and to thermal stress in general). Apparatus for experimental evaluation of thermal shock resistance is available in only a few places, and is normally specialized to one or a few specific specimen sizes and shapes. So far as is known, none of these specimen geometries happens to be appropriate for evaluating the small specimens which CMF-13 usually produces.

Certain of the experimental graphites produced by CMF-13 are expected to have unusually high resistance to thermal shock, and low thermal-shock resistance is expected to be an important limitation of certain others. Since little confidence is placed in calculated thermal shock indices, and since apparatus for experimentally evaluating thermal shock resistance of these materials is apparently not available elsewhere, it seems important that CMF-13 develop a testing capability of its own. Such a development has therefore been undertaken, on a relatively low priority (because CMF-13 manpower for such work is limited). The apparatus used is an electron-beam gun, in a system designed to test specimens approximately 0.5 in. dia. -- such as can be machined from the extruded graphite rods normally made by the Group. In preliminary experiments on seven widely different graphites, all were

broken at a specimen thickness of 0.033 in., and a wide range of power was required. Commercial AGSX and one CMF-13 experimental graphite broke at 400 watts power input, while 1820 watts were required to crack commercial 886-S and a different experimental grade. In common with other apparatus using an intense heat source, such as an electric arc, this electron gun appears to deposit too much energy at the center of the heated spot on the specimen surface. Here it rapidly vaporizes the graphite, and often penetrates the specimen completely. Attempts to spread the energy over a larger area by defocussing the electron beam have been partially successful, and cracking has been produced in the specimens tested. However, defocussing has resulted in a nonuniform pattern of energy-deposition. A redesigned electron gun and deflection system, capable of higher power and better control, has therefore been built and will soon be tested in this apparatus.

A testing unit of this type has obvious advantages and limitations. It is potentially capable of precise control of both energy input to the specimen and of energy distribution on the specimen surface. Operating in a vacuum it provides for removal of moisture and adsorbed gases from the specimen before it is tested, and it can be used to preheat specimens either to degas them thoroughly or to initiate thermal shock tests at an elevated temperature rather than at ambient temperature. With a good vacuum system and a rotating specimen table, it permits reasonably rapid testing. In its present state it is intended to be used only on small-diameter specimens, although it could be modified for larger ones. To be broken in thermal stress, a specimen of small diameter must also be relatively thin, and a thickness of about 0.033 in. seems to be suitable at 0.5 in. diameter. To be reliable with this specimen geometry, testing must probably be confined to carbons and graphites in which maximum filler-particle diameter is small compared to 0.033 in., which limits it to tests on very fine-grained materials.

APPENDIX

PUBLICATIONS RELATING TO CARBONS AND GRAPHITES

PROGRESS REPORTS:

Smith, M. C., CMF-13 Research on Carbon and Graphite,

"Report No. 1, Summary of Progress to May 1, 1967", LASL Report No. LA-3693-MS. Distributed June 1, 1967. 20 p.

"Report No. 2, Summary of Progress from May 1 to July 31, 1967", LASL Report No. LA-3758-MS. Distributed September 15, 1967. 20 p.

"Report No. 3, Summary of Progress from August 1 to October 31, 1967", LASL Report No. LA-3821-MS. Distributed November 15, 1967. 24 p.

"Report No. 4, Summary of Progress from November 1, 1967, to January 31, 1968", LASL Report No. LA-3872-MS. Distributed February 9, 1968. 25 p.

"Report No. 5, Summary of Progress from February 1 to April 30, 1968", LASL Report No. LA-3932-MS. Distributed May 20, 1968. 38 p.

"Report No. 6, Summary of Progress from May 1 to July 31, 1968", LASL Report No. LA-3989-MS. Distributed September 4, 1968. 33 p.

TOPICAL REPORTS:

Merryman, R. G., Wagner, P., and MacMillan, D. P., "H4LM Graphite Review", LASL Report No. LAMS-2725, September, 1962.

Lewis, H. D., and Moore, R. H., "On the Proper Use of Transformations of Log Normal Functions in Small Particle Statistics", LASL Report No. LA-3262, July, 1965.

Bard, R. J., O'Rourke, J. A., et al, "Development of Particles Coated with Pyrolytic Carbon, I ", LASL Report No. LA-3496, January, 1967.

Bard, R. J., O'Rourke, J. A., et al, "Development of Particles Coated with Pyrolytic Carbon, II ", LASL Report No. LA-3601, March, 1967.

Bard, R. J., O'Rourke, J. A., et al, "Development of Particles Coated with Pyrolytic Carbon, III ", LASL Report No. LA-3660, June, 1967.

Eash, D. T., "Cryogenic Thermal Expansion of Y-12 Graphite Fuel Elements", (CONF. RD), LASL Report No. LA-3857, January, 1968.

Dickinson, J. M. and Lewis, H. D., "Porosimetry Data Interpretation", LASL Report No. LA-3938, June, 1968.

Imprescia, R. J., "Estimation of Optimum Binder Concentration for Molded Carbons", LASL Report No. LA-3901, August, 1968.

Smith, M. C., "The Manufacture and Properties of an Extruded, Resin-Bonded Graphite, CMF-13 Lot AAQ1", LASL Report No. LA-3981, October, 1968.

Lewis, H. D., and Goldman, A., "Theoretical Small-Particle Statistics; A Summary of Techniques for Data Analysis with Recent Developments in Data Comparison, Notation, and Mixture Theory", LASL Report No. LA-3656, November, 1968.

JOURNAL PUBLICATIONS:

Driesner, A. R., and Wagner, P., "Friction Coefficients of Graphite from 25°C to 2450°C", J. Appl. Phys., 29, 901 (1958).

Wagner, P., Driesner, A. R., and Kmetko, E. A., "Mechanical Properties of Graphite from 20°C to 3000°C", Proc. 2nd Int. Conf. on Uses of Atomic Energy, 702 (1958).

Wagner, P., and Driesner, A. R., "High Temperature Graphite; Creep in Compression", J. Appl. Phys., 30, 148 (1959).

Wagner, P., Driesner, A. R., and Haskin, L. A., "High Temperature Graphite; Creep in Tension", J. Appl. Phys., 30, 152 (1959).

Brown, H. L., and Armstrong, P. E., "Young's Modulus Measurements Above 2000°C", RSI, 6, 636 (1963).

Armstrong, P. E., and Brown, H. L., "Dynamic Young's Modulus Measurements Above 1000°C on Some Pure Polycrystalline Metals and Commercial Graphites", Trans. AIME, 230, 962 (1964).

Smith, M. C., "Effects of Temperature and Strain Rate on Transverse Tensile Properties of H4LM Graphite Tested in Helium and in Vacuum", Carbon, 1, 147 (1964).

Smith, M. C., Eash, D. T., and McKibbin, K., "Longitudinal Tensile Properties of H4LM Graphite in the Temperature Range -253° to 500°C", Carbon, 1, 181 (1964).

Smith, M. C., "Effects of Prestrain on the Tensile Properties of Graphite", Carbon, 2, 269 (1964).

Smith, M. C., "Longitudinal Tensile Behavior of H4LM Graphite in Nitrogen to 2750°C", J. Nucl. Mat., 13, 57 (1964).

Smith, M. C., "Time-Dependent Strengthening of Graphite in Tension at 2500°C", Carbon, 3, 96 (1965).

Eash, D. T., "Longitudinal Tensile Properties of H4LM Graphite Extended to -269°C", Carbon, 3, 97 (1965).

Lewis, H. D., and Goldman, A., "Proper Analysis of Coulter Counter Data", RSI, 36, 868 (1965).

Green, W. V., "The Stress Dependence of the Creep Rate of a Uranium-Loaded Graphite", Carbon, 4, 81 (1966).

Zukas, E. G., and Green, W. V., "Dependence of Rate of Creep on the Orientation of the Tensile Axis for Heavily Oriented Graphite", Nature, 212, 1454 (1966).

Lewis, H. D., and Goldman, A., "Theorems for Calculation of Weight Ratios to Produce Maximum Packing Density of Powder Mixtures", J. Am. Cer. Soc., 49, 323 (1966).

Reiswig, R. D., Lewis, H. D., and Baker, T. D., "Microscopic Examination of Powders", RSI, 37, 376 (1966).

Wagner, P., "A Versatile High Temperature Furnace", RSI, 37, 1054 (1966).

Green, W. V., and Zukas, E. G., "The Stress Dependence of the Creep Rate of Two Commercial Graphites", Electrochem. Techn., 5, 203 (1967).

Green, W. V., Levinson, L. S., and Zukas, E. G., "A Method for Determining the Microstructural Changes in Graphite That Accompany High Temperature Deformation", Carbon, 5, 583 (1967).

Reiswig, R. D., Levinson, L. S., and Baker, T. D., "Optical and Electron Microscopy of Carbonaceous

Materials", Carbon, 5, 603 (1967).

Wagner, P., and Daucisberg, L. B., "Thermal Conductivity of ZTA Graphite", Carbon, 5, 271 (1967).

Zukas, F. G., and Green, W. V., "The High-Temperature Creep Behavior of a Highly-Oriented Polycrystalline Graphite", Carbon, 6, 101 (1968).

Reiswig, R. D., Levinson, L. S., and O'Rourke, J. A., "Graphitization of Polyfurfuryl Alcohol", Carbon, 6, 124 (1968).

Wewerka, E. M., "The Determination of the Molecular Distributions of Graphite Binder Materials by Gel Permeation Chromatography", Carbon, 6, 93 (1968).

Wagner, P., and Daucisberg, L. B., "The Thermal Conductivity of SX-5 Graphite", Carbon, 6, 373 (1968).

Impresela, R. J., Wagner, P., and O'Rourke, J. A., "The Effects of Curing and Baking Environments on Properties of Some Molded Graphites", Carbon, 6, 421 (1968).

Wewerka, E. M., "An Investigation of the Polymerization of Furfuryl Alcohol with Gel Permeation Chromatography", J. Appl. Poly. Sci., 12, 1671 (1968).

Smith, M. C., "Relaxation of Tensile Stress in a Reactor Graphite at 2000° to 2700°C", Carbon, 6, 503 (1968).

Wagner, P., and Daucisberg, L. B., "Some Thermal Properties of a Polyfurfuryl Alcohol Bonded Graphite", Carbon (in Press).

Wagner, P., "On the Technique of Measuring the High Temperature Thermal Conductivity of a Rod", British J. Appl. Phys. (in Press).